Analysis of three-body charmless B-meson decays under the factorization-assisted topological-amplitude approach

Si-Hong Zhou,* Xin-Xia Hai, and Run-Hui Li†

School of Physical Science and Technology, Inner Mongolia University, Hohhot 010021, China

Cai-Dian Lü‡

Institute of High Energy Physics, CAS, Beijing 100049, China and School of Physics, University of Chinese Academy of Sciences, Beijing 100049, China

(Received 8 May 2023; accepted 13 June 2023; published 28 June 2023)

We analyze quasi-two-body charmless B decays $B_{(s)} \to P_1V \to P_1P_2P_3$ with V representing a vector resonant, and $P_{1,2,3}$ as a light pseudoscalar meson, pion, kaon, or $\eta^{(\prime)}$. The intermediate processes $B_{(s)} \to P_1V$ are calculated in the factorization-assisted topological-amplitude approach and the vector resonant effects are described by the Breit-Wigner propagator, which successively decay to P_1P_2 via strong interaction. Taking into account of all vector resonances in ground state, ρ, K^*, ω, ϕ, we present the related branching fractions, and calculate the virtual effects for $B_{(s)} \to \pi, K(\rho, \omega \to)KK$. We also predict direct CP asymmetries of three-body B decay modes with ρ, K^* resonances as intermediate states. Our predicted branching fractions of decay modes dominated by the color-favored tree diagram or the color-favored penguin diagram are consistent with the perturbative QCD approach's predictions as well as the QCD factorization approach. While for those nonperturbative contribution dominated decay modes, the branching ratios in this work are in better agreement with current experimental data than the perturbative QCD (PQCD) predictions and the QCD factorization results due to their shortage of the nonperturbative contributions or $1/m_b$ power corrections. Many of the decays channels, especially for direct CP asymmetries, are waiting for the future experiments.

DOI: 10.1103/PhysRevD.107.116023

I. INTRODUCTION

Three-body nonleptonic B meson decays constitute a large portion of B decay channels. Contrary to two-body B meson decays, they have nontrivial kinematics and phase space distributions, which can provide more opportunities for the study of CP asymmetries and factorization issues in QCD for multibody nonleptonic decays. Generally, one can utilize the Dalitz plot technique to analyze the phase space of three-body B meson decays, where the invariant mass of a pair of final-state particles peaks as a resonance. In the edges of the Dalitz plot, various resonances as the intermediate states in three-body B meson decays will show up, so that the analysis on these decays enables one to study the properties of these resonances.

Experimentally, a large amount of branching ratios and CP asymmetry parameters of three-body charmless B decays have already been measured by *BABAR*, Belle, and LHCb collaborations [1–5], while more are expected from the upgrade of LHCb and Belle II experiments. On the theoretical side, three-body nonleptonic B meson decays are more complicated than two-body cases as they involve three-body decay matrix elements. In a phenomenological factorization model [6–8], the three-body matrix elements of charmless B decays were factorized naively, with the resulting local correlaters studied extensively based on heavy meson chiral perturbation theory for nonresonant contributions and the usual Breit-Wigner formalism for resonant effects. Besides these phenomenological descriptions of three-body charmless B decays in the whole Dalitz plot, theoretical analysis in the context of QCD factorization are mainly concentrated on the edges of the Dalitz distribution, since the contribution in the center regions of phase space is argued to be both $1/m_b$ power and α_s suppressed [9,10].

Since the vector (scalar) mesons usually decay dominantly to two pseudoscalar mesons with large decay width, the three-body B decays are found to be dominantly

*shzhou@imu.edu.cn
†lirh@imu.edu.cn
‡lucd@ihep.ac.cn

happened by B decaying to a vector (scalar) meson and a pseudoscalar meson, and the vector (scalar) meson subsequently decaying to two pseudoscalar mesons. In this case, two of the three final particles are collinear, generating a small invariant mass in the edges of the Dalitz distribution, and recoil against the third meson in three-body decays. Then one expects a similar factorization theorem as for two-body decays, with the difference that one of the mesons in the two-body case is substituted by a pair of collinear moving mesons with small invariant mass. A series of works [10–22] using perturbative QCD approach concentrated on this situation that the pair of collinear mesons are described collectively through intermediate resonances, that is, the three-body decays are processed as quasi-two-body decays. The CP asymmetry of $B \to \pi\pi\pi$ decays has been studied within the QCD factorization framework at leading order in α_s [23,24], using naive factorization for three-body matrix elements, which involve the generalized form factor of $B \to \pi\pi$ transition and dimension light cone distribution amplitudes in [25–28]. The calculation of the nonleptonic three-body B decays with heavy-to-heavy transitions, up to the precision of next-next-to-leading order in α_s has also been done in QCD factorization [29]. In all these quasi-two-body calculations of the three-body B decays, the theoretical calculations rely heavily on the precision of two-body theoretical calculation methods.

In the case of two-body nonleptonic B decays, power corrections in the heavy-quark expansion, such as weak annihilation effects and chirally enhanced power corrections, are difficult to estimate and remain the sources of uncertainty in QCD factorization approach [30]. A complete next-to-leading order calculation of two-body B decays in perturbative QCD factorization approach has not been finished [31]. The problem about precision predictions in the calculation of two-body nonperturbative matrix elements also exist in the three-body case. As discussed in Ref. [8], the predicted branch ratios of quasi-two-body decays such as $B \to \phi(K^+K^-)K, K^*(K^-\pi^+)\pi, \rho(\pi^+\pi^-)K$ are smaller than experimental data due to the absence of $1/m_b$ power corrections. To include the nonperturbative and nonfactorization contribution in two-body B decays, a model independent framework of topological diagram approach [32] has been introduced. The equivalence of the topological decay amplitudes and the $SU(3)$ irreducible amplitudes has been approved [33,34]. In this approach, one classifies the decay amplitudes of two-body charmless B decays into different electroweak topological Feynman diagrams under $SU(3)$ symmetry. The topological amplitudes including the nonfactorizable QCD contributions were extracted through a global fit from all experimental data of these decays. The precision of this topological diagram approach is limited to the size of $SU(3)$ breaking effect.

In order to include the $SU(3)$ breaking effects, the so-called factorization-assisted topological-amplitude (FAT) approach [35–42] has been introduced. They can give the most precise decay amplitudes of the two-body charmless B-meson decays. For instance, the amplitude of the color-suppressed topological diagram dominated by the nonfactorizable QCD effect, was larger in the FAT approach than that in other perturbative approaches so that the long-standing $B \to \pi\pi$ branching ratio puzzle and $B \to \pi K$ CP asymmetry puzzle were solved simultaneously. Encouraged by the success in two-body B decays, we will systematically analyze three-body charmless B decays using the FAT approach at the edges of the Dalitz distribution with only vector resonance contribution, i.e., quasi-two-body decays with two of the pseudoscalar mesons decaying from the vector resonance. The vector resonant effects are described in terms of the usual Breit-Wigner formalism, and a strong coupling accounts for the subsequent vector meson two-body decay. We will study the branching ratios and CP violations of these three-body B decays, and discuss the virtual effects of intermediate resonance ρ, K^*, ω, and ϕ on quasi-two-body decays.

This paper is organized as follows. In Sec. II, the theoretical framework is introduced. The numerical results and discussions are collected in Sec. III. Section V is a summary.

II. FACTORIZATION AMPLITUDES FOR TOPOLOGICAL DIAGRAMS

As a quasi-two-body process, the $B_{(s)} \to P_1P_2P_3$ decay (with P denoting a light pseudoscalar meson) is divided into two stages. First, $B_{(s)}$ meson decays to P_1V, and the intermediate vector resonance V decays to P_2P_3 subsequently. The first decay $B_{(s)} \to P_1V$ is a weak decay induced by $b \to u\bar{u}d(s)$ at quark level in leading order (tree diagram) and $b \to d(s)q\bar{q}(q = u, d, s)$ in next-to-leading order (penguin loop diagram). The secondary decay $V \to P_2P_3$ proceeds via strong interaction. In Fig. 1 we show the topological diagrams of $B_{(s)} \to P_1P_2P_3$ under the framework of quasi-two-body decay at tree level, including (i) color-favored tree emission diagram T, (ii) color-suppressed tree emission diagram C, (iii) W-exchange tree diagram E, and (iv) W-annihilation tree diagram A, which are specified by topological structures of the weak interaction. Likewise, one loop penguin diagram can also be grouped into four categories: (i) QCD-penguin emission diagram P, (ii) flavor-singlet QCD-penguin diagram P_C or EW-penguin emission diagram P_{EW}, (iii) timelike QCD-penguin diagram P_E, and (iv) spacelike QCD-penguin annihilation diagram P_A, which are shown in Fig. 2. In the two kinds of figures, we only show one case that the intermediate resonance (labeled by gray ovals) is produced as a recoiling particle in emission diagrams.

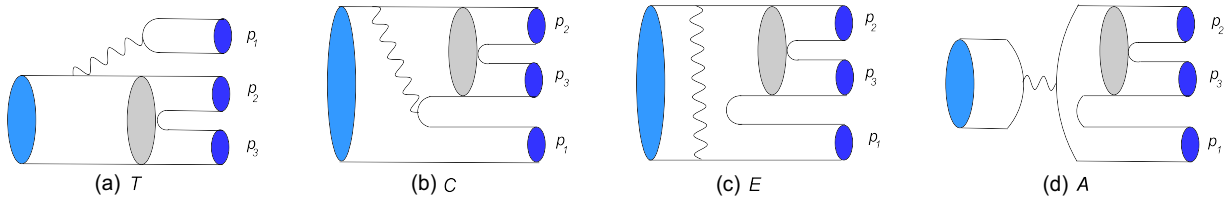

FIG. 1. Typical topological tree diagrams of $B_{(s)} \to P_1V \to P_1P_2P_3$ under the framework of quasi-two-body decay with the wavy line representing a W boson: (a) color-favored tree diagram T, (b) color-suppressed tree diagram C, (c) W-exchange tree diagram E, and (d) W-annihilation tree diagram A.

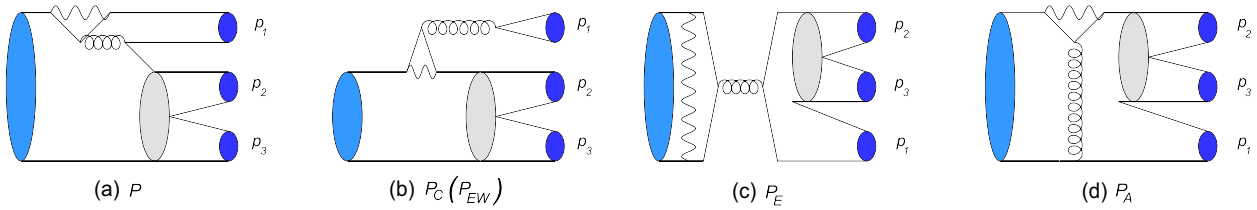

FIG. 2. Typical topological penguin diagrams of $B_{(s)} \to P_1V \to P_1P_2P_3$ under the framework of quasi-two-body decay with the wavy line representing a W boson: (a) QCD-penguin emission diagram P, (b) flavor-singlet QCD-penguin diagram P_C or EW-penguin diagram $P_{\rm EW}$, (c) timelike QCD-penguin diagram P_E, and (d) spacelike QCD-penguin annihilation diagram P_A.

The electroweak B decays at tree level have been proven to be factorizable at high precision [43]. Therefore, we can calculate the decay amplitude of color-favored tree diagram T in perturbative QCD order by order. Large nonfactorizable contributions, such as soft corrections to the color-suppressed tree amplitude and $1/m_b$ power corrections from annihilation type diagram, are found to be non-negligible [38]. Similar to the FAT approach for two-body B decays [38], we have to introduce unknown parameters for nonfactorizable contributions for color-suppressed tree diagram C, and W-exchange tree diagram E (W-annihilation tree diagram A is negligible) to be fitted from experimental data. The formulas of $B_{(s)} \to P_1V, VP_1$ decays are given as [38]

$$\begin{aligned}
T^{P_1V} &= \sqrt{2}G_F V_{ub}V^*_{uq'}a_1(\mu)f_V m_V F_1^{B-P_1}(m_V^2)(\varepsilon_V^*\cdot p_B),\\
T^{VP_1} &= \sqrt{2}G_F V_{ub}V^*_{uq'}a_1(\mu)f_{P_1} m_V A_0^{B-V}(m_{P_1}^2)(\varepsilon_V^*\cdot p_B),\\
C^{P_1V} &= \sqrt{2}G_F V_{ub}V^*_{uq'}\chi^{C'}e^{i\phi^{C'}}f_V m_V F_1^{B-P_1}(m_V^2)(\varepsilon_V^*\cdot p_B),\\
C^{VP_1} &= \sqrt{2}G_F V_{ub}V^*_{uq'}\chi^{C}e^{i\phi^{C}}f_{P_1} m_V A_0^{B-V}(m_{P_1}^2)(\varepsilon_V^*\cdot p_B),\\
E^{P_1V,VP_1} &= \sqrt{2}G_F V_{ub}V^*_{uq'}\chi^{E}e^{i\phi^{E}}f_B m_V\left(\frac{f_{P_1}f_V}{f_\pi^2}\right)(\varepsilon_V^*\cdot p_B).
\end{aligned} \tag{1}$$

The QCD-penguin emission diagram P and the electroweak penguin emission diagram $P_{\rm EW}$ are also proved to be factorizable, and thus are calculable in QCD factorization. The flavor-singlet QCD-penguin diagram P_C and spacelike QCD-penguin annihilation diagram P_A contain large nonfactorizable contribution which will be determined by χ^2 fit from experimental data. The timelike QCD-penguin diagram P_E is found to be smaller than other contribution, which can be ignored in the modes not dominated by it in the fit as discussed in [38]. The formulas can be expressed as [38]

$$\begin{aligned}
P^{P_1V} &= -\sqrt{2}G_F V_{tb}V^*_{tq'}a_4(\mu)f_V m_V F_1^{B-P_1}(m_V^2)(\varepsilon_V^*\cdot p_B),\\
P^{VP_1} &= -\sqrt{2}G_F V_{tb}V^*_{tq'}[a_4(\mu)-\chi^{P}e^{i\phi^{P}}r_\chi]f_{P_1} m_V A_0^{B-V}(m_{P_1}^2)(\varepsilon_V^*\cdot p_B),\\
P_C^{P_1V} &= -\sqrt{2}G_F V_{tb}V^*_{tq'}\chi^{P'_C}e^{i\phi^{P'_C}}f_V m_V F_1^{B-P_1}(m_V^2)(\varepsilon_V^*\cdot p_B),\\
P_C^{VP_1} &= -\sqrt{2}G_F V_{tb}V^*_{tq'}\chi^{P_C}e^{i\phi^{P_C}}f_{P_1} m_V A_0^{B-V}(m_{P_1}^2)(\varepsilon_V^*\cdot p_B),\\
P_A^{P_1V} &= -\sqrt{2}G_F V_{tb}V^*_{tq'}\chi^{P_A}e^{i\phi^{P_A}}f_B m_V\left(\frac{f_{P_1}f_V}{f_\pi^2}\right)(\varepsilon_V^*\cdot p_B),
\end{aligned} \tag{2}$$

$$P_{\rm EW}^{P_1V} = -\frac{3\sqrt{2}}{2} G_F V_{tb} V_{tq'}^* e_q a_9(\mu) f_V m_V F_1^{B-P_1}(m_V^2)(\varepsilon_V^* \cdot p_B),$$
$$P_{\rm EW}^{VP_1} = -\frac{3\sqrt{2}}{2} G_F V_{tb} V_{tq'}^* e_q a_9(\mu) f_{P_1} m_V A_0^{B-V}(m_{P_1}^2)(\varepsilon_V^* \cdot p_B). \quad (3)$$

In these equations, we use the superscripts P_1V, VP_1 to distinguish cases in which the recoiling meson (the first particle of P_1V, VP_1) is a pseudoscalar or a vector meson. The quark in the Cabibbo-Kobayashi-Maskawa (CKM) matrix element is $q' = d, s$. ε_V^* is the polarization vector of vector meson V. $r_\chi = \frac{m_{P_1}^2}{m_{q'} m_B}$ is the chiral factor of pseudoscalar meson in the "chiral enhanced" term of P^{VP_1} amplitude. f_{P_1}, f_V are the decay constants of the corresponding meson P_1 and V. $F_1^{B-P_1}$ and A_0^{B-V} represent the vector form factors of $B_{(s)} \to P_1$ and $B_{(s)} \to V$ transitions. The Q^2 dependent of form factor is expressed in the dipole model as

$$F_i(Q^2) = \frac{F_i(0)}{1 - \alpha_1 \frac{Q^2}{m_{\rm pole}^2} + \alpha_2 \frac{Q^4}{m_{\rm pole}^4}}, \quad (4)$$

where F_i represents form factor F_1 or A_0, and $m_{\rm pole}$ is the mass of the corresponding pole state, e.g., B for A_0, and B^* for F_1. The effective Wilson coefficients $a_i(\mu)$ can be calculated perturbatively. $\chi^{C^{(\prime)}(E,P,P_C^{(\prime)},P_A)}$ and $\phi^{C^{(\prime)}(E,P,P_C^{(\prime)},P_A)}$ denote the magnitude and associate phase of C (E, P, P_C, and P_A) diagram, which are universal to be fitted globally from the experimental data.

We adopt the relativistic Breit-Wigner line shape to describe ρ, K^*, ω, and ϕ resonances, which is widely used in the experimental data analyses [44–46]. The explicit expression of relativistic Breit-Wigner line shape is in the following form:

$$L^{\rm RBW}(s) = \frac{1}{s - m_V^2 + i m_V \Gamma_V(s)}, \quad (5)$$

where the two-body invariant mass square is $s = m_{23}^2 = (p_2 + p_3)^2$ with p_2 and p_3 denoting the 4-momenta of the collinearly moving mesons P_2 and P_3, respectively. The energy-dependent width of vector resonance $\Gamma_V(s)$ is defined by

$$\Gamma_V(s) = \Gamma_0 \left(\frac{q}{q_0}\right)^3 \left(\frac{m_V}{\sqrt{s}}\right) X^2(q r_{\rm BW}). \quad (6)$$

The Blatt-Weisskopf barrier factor $X(q r_{\rm BW})$ is given as [47]

$$X(q r_{\rm BW}) = \sqrt{[1 + (q_0 r_{\rm BW})^2]/[1 + (q r_{\rm BW})^2]}, \quad (7)$$

where $q = \frac{1}{2}\sqrt{[s - (m_{P_2} + m_{P_3})^2][s - (m_{P_2} - m_{P_3})^2]/s}$ is the magnitude of the momentum of the final state P_2 or P_3 in the rest frame of resonance V, and q_0 is the value of q when $s = m_V^2$. When a pole mass locates outside the kinematics region, i.e., $m_V < m_{P_2} + m_{P_3}$, m_V will be replaced with an effective mass $m_V^{\rm eff}$, given by the *ad hoc* formula [48,49],

$$m_V^{\rm eff}(m_V) = m^{\rm min} + (m^{\rm max} - m^{\rm min}) \times \left[1 + \tanh\left(\frac{m_V - \frac{m^{\rm min} + m^{\rm max}}{2}}{m^{\rm max} - m^{\rm min}}\right)\right], \quad (8)$$

where $m^{\rm max}$ and $m^{\rm min}$ are the upper and lower boundaries of the kinematics region, respectively. The barrier radius $r_{\rm BW} = 4.0\ ({\rm GeV})^{-1}$ is for all resonances [46]. The full widths of the resonances Γ_0, together with their masses m_V, are taken from Particle Data Group [50] and listed in Table I.

TABLE I. Masses m_V and full widths Γ_0 of vector resonant states.

Resonance	Line shape parameters	Resonance	Line shape parameters
$\rho(770)$	$m_V = 775.26$ MeV, $\Gamma_0 = 149.1$ MeV	$\omega(782)$	$m_V = 782.65$ MeV, $\Gamma_0 = 8.49$ MeV
$K^*(892)^+$	$m_V = 891.66$ MeV, $\Gamma_0 = 50.8$ MeV	$K^*(892)^0$	$m_V = 895.55$ MeV, $\Gamma_0 = 47.3$ MeV
$\phi(1020)$	$m_V = 1019.46$ MeV, $\Gamma_0 = 4.25$ MeV		

The matrix element of strong decay $\langle P_2(p_2)P_3(p_3)|V(p_V)\rangle$ is parametrized as a strong coupling constant $g_{VP_2P_3}$, which can be extracted from measured the partial decay widths $\Gamma_{V\to P_2P_3}$ through the relations

$$\Gamma_{V\to P_2P_3} = \frac{2}{3}\frac{p_c^3}{4\pi m_V^2} g_{V\to P_2P_3}^2, \quad (9)$$

where p_c is the magnitude of pseudoscalar meson momentum in the rest frame of vector meson. The numerical results of $g_{\rho\to\pi^+\pi^-}$, $g_{K^*\to K^+\pi^-}$, and $g_{\phi\to K^+K^-}$ have already been determined from experimental data [8],

$$g_{\rho\to\pi^+\pi^-} = 6.0, \quad g_{K^*\to K^+\pi^-} = 4.59, \quad g_{\phi\to K^+K^-} = -4.54. \quad (10)$$

The other strong coupling constants can be derived from the relationships with the results in Eq. (10) by using the quark model result [51],

$$g_{\rho\to K^+K^-} : g_{\omega\to K^+K^-} : g_{\phi\to K^+K^-} = 1 : 1 : -\sqrt{2},$$
$$g_{\rho^0\pi^+\pi^-} = g_{\rho^+\pi^0\pi^+}, \quad g_{\rho^0\pi^0\pi^0} = g_{\omega\pi^+\pi^-} = 0,$$
$$g_{\rho^0K^+K^-} = -g_{\rho^0K^0\bar{K}^0} = g_{\omega K^+K^-} = g_{\omega K^0\bar{K}^0},$$
$$g_{\phi K^+K^-} = g_{\phi K^0\bar{K}^0}.$$

Combing them together for quasi-two-body decay $B_{(s)} \to P_1 V \to P_1 P_2 P_3$, we express the decay amplitudes of tree topological diagrams shown in Fig. 1 as

$$\begin{aligned}
T^{(P_2P_3)P_1} &= \langle P_2(p_2)P_3(p_3)|(\bar{u}b)_{V-A}|B(p_B)\rangle\langle P_1(p_1)|(\bar{q}u)_{V-A}|0\rangle, \\
&= \frac{\langle P_2(p_2)P_3(p_3)|V(p_V)\rangle}{s-m_V^2+im_V\Gamma_V(s)}\langle V(p_V)|(\bar{u}b)_{V-A}|B(p_B)\rangle\langle P_1(p_1)|(\bar{q}u)_{V-A}|0\rangle, \\
&= p_1\cdot(p_2-p_3)\sqrt{2}G_F V_{ub}V_{uq'}^* a_1(\mu) f_{P_1} m_V A_0^{BV}(m_{P_1}^2)\frac{g_{VP_2P_3}}{s-m_V^2+im_V\Gamma_V(s)}, \\
T^{P_1(P_2P_3)} &= \langle P_2(p_2)P_3(p_3)|(\bar{q}u)_{V-A}|0\rangle\langle P_1(p_1)|(\bar{u}b)_{V-A}|B(p_B)\rangle, \\
&= \frac{\langle P_2(p_2)P_3(p_3)|V(p_V)\rangle}{s-m_V^2+im_V\Gamma_V(s)}\langle V(p_V)|(\bar{q}u)_{V-A}|0\rangle\langle P_1(p_1)|(\bar{u}b)_{V-A}|B(p_B)\rangle, \\
&= p_1\cdot(p_2-p_3)\sqrt{2}G_F V_{ub}V_{uq'}^* a_1(\mu) f_V m_V F_1^{BP_1}(s)\frac{g_{VP_2P_3}}{s-m_V^2+im_V\Gamma_V(s)},
\end{aligned} \tag{11}$$

$$\begin{aligned}
C^{(P_2P_3)P_1} &= \langle P_2(p_2)P_3(p_3)|(\bar{u}b)_{V-A}|B(p_B)\rangle\langle P_1(p_1)|(\bar{q}u)_{V-A}|0\rangle, \\
&= \frac{\langle P_2(p_2)P_3(p_3)|V(p_V)\rangle}{s-m_V^2+im_V\Gamma_V(s)}\langle V(p_V)|(\bar{u}b)_{V-A}|B(p_B)\rangle\langle P_1(p_1)|(\bar{q}u)_{V-A}|0\rangle, \\
&= p_1\cdot(p_2-p_3)\sqrt{2}G_F V_{ub}V_{uq'}^* \chi^C e^{i\phi^C} f_{P_1} m_V A_0^{BV}(m_{P_1}^2)\frac{g_{VP_2P_3}}{s-m_V^2+im_V\Gamma_V(s)}, \\
C^{P_1(P_2P_3)} &= \langle P_2(p_2)P_3(p_3)|(\bar{q}u)_{V-A}|0\rangle\langle P_1(p_1)|(\bar{u}b)_{V-A}|B(p_B)\rangle, \\
&= \frac{\langle P_2(p_2)P_3(p_3)|V(p_V)\rangle}{s-m_V^2+im_V\Gamma_V(s)}\langle V(p_V)|(\bar{q}u)_{V-A}|0\rangle\langle P_1(p_1)|(\bar{u}b)_{V-A}|B(p_B)\rangle, \\
&= p_1\cdot(p_2-p_3)\sqrt{2}G_F V_{ub}V_{uq'}^* \chi^{C'} e^{i\phi^{C'}} f_V m_V F_1^{BP_1}(s)\frac{g_{VP_2P_3}}{s-m_V^2+im_V\Gamma_V(s)},
\end{aligned} \tag{12}$$

$$\begin{aligned}
E^{P_1(P_2P_3)} &= \langle P_1(p_1)P_2(p_2)P_3(p_3)|\mathcal{H}_{\rm eff}|B(p_B)\rangle, \\
&= \frac{\langle P_2(p_2)P_3(p_3)|V(p_V)\rangle}{s-m_V^2+im_V\Gamma_V(s)}\langle V(p_V)P_1(p_1)|\mathcal{H}_{\rm eff}|B(p_B)\rangle, \\
&= p_1\cdot(p_2-p_3)\sqrt{2}G_F V_{ub}V_{uq'}^* \chi^E e^{i\phi^E} f_B m_V \frac{f_V f_{P_1}}{f_\pi^2}\frac{g_{VP_2P_3}}{s-m_V^2+im_V\Gamma_V(s)},
\end{aligned} \tag{13}$$

where $q' = d,\ s$ and $p_V = p_2 + p_3 = \sqrt{s}$. Similarly, the amplitudes of penguin diagrams shown in Fig. 2 can be expressed as

$$\begin{aligned}
P^{(P_2P_3)P_1} &= -p_3\cdot(p_1-p_2)\sqrt{2}G_F V_{tb}V_{tq'}^*[a_4(\mu)-\chi^P e^{i\phi^P} r_\chi] f_{P_3} m_V A_0^{BV}(m_{P_3}^2)\frac{g_{VP_1P_2}}{s-m_V^2+im_V\Gamma_V(s)}, \\
P^{P_1(P_2P_3)} &= -p_3\cdot(p_1-p_2)\sqrt{2}G_F V_{tb}V_{tq'}^* a_4(\mu) f_V m_V F_1^{BP_1}(s)\frac{g_{VP_1P_2}}{s-m_V^2+im_V\Gamma_V(s)}, \\
P_A^{P_1(P_2P_3)} &= -p_1\cdot(p_2-p_3)\sqrt{2}G_F V_{tb}V_{tq'}^* \chi^{P_A} e^{i\phi^{P_A}} f_B m_V \frac{f_V f_{P_1}}{f_\pi^2}\frac{g_{VP_2P_3}}{s-m_V^2+im_V\Gamma_V(s)}, \\
P_C^{(P_2P_3)P_1} &= -p_1\cdot(p_2-p_3)\sqrt{2}G_F V_{tb}V_{tq'}^* \chi^{P_C} e^{i\phi^{P_C}} f_{P_1} m_V A_0^{BV}(m_{P_1}^2)\frac{g_{VP_2P_3}}{s-m_V^2+im_V\Gamma_V(s)}, \\
P_C^{P_1(P_2P_3)} &= -p_1\cdot(p_2-p_3)\sqrt{2}G_F V_{tb}V_{tq'}^* \chi^{P'_C} e^{i\phi^{P'_C}} f_V m_V F_1^{BP_1}(s)\frac{g_{VP_2P_3}}{s-m_V^2+im_V\Gamma_V(s)}, \\
P_{\rm EW}^{(P_2P_3)P_1} &= -p_1\cdot(p_2-p_3)\frac{3\sqrt{2}}{2}G_F V_{tb}V_{tq'}^* e_q a_9(\mu) f_{P_1} m_V A_0^{BV}(m_{P_1}^2)\frac{g_{VP_2P_3}}{s-m_V^2+im_V\Gamma_V(s)}, \\
P_{\rm EW}^{P_1(P_2P_3)} &= -p_1\cdot(p_2-p_3)\frac{3\sqrt{2}}{2}G_F V_{tb}V_{tq'}^* e_q a_9(\mu) f_V m_V F_1^{BP_1}(s)\frac{g_{VP_2P_3}}{s-m_V^2+im_V\Gamma_V(s)},
\end{aligned} \tag{14}$$

where the form factor $F_1^{BP_1}$ is dependent on invariant mass s not a fixed value as in two-body decays.

TABLE II. Decay constants of light pseudoscalar mesons and vector mesons (in units of MeV).

f_π	f_K	f_B	f_ρ	f_{K^*}	f_ω	f_ϕ
130.2 ± 1.7	155.6 ± 0.4	190.9 ± 4.1	213 ± 11	220 ± 11	192 ± 10	225 ± 11

The matrix element of $B_{(s)} \to P_1P_2P_3$ can be written in the following form:

$$\langle P_1(p_1)P_2(p_2)P_3(p_3)|\mathcal{H}_{\rm eff}|B_{(s)}(p_B)\rangle = p_1\cdot(p_2-p_3)\mathcal{A}(s), \tag{15}$$

where $\mathcal{A}(s)$ represents the summation of amplitudes in Eqs. (11)–(13) and Eq. (14) with the prefactor $p_1\cdot(p_2-p_3)$ taken out. The differential width of $B_{(s)} \to P_1P_2P_3$ is

$$d\Gamma = ds\frac{1}{(2\pi)^3}\frac{(|\mathbf{p}_1||\mathbf{p}_2|)^3}{6m_B^3}|\mathcal{A}(s)|^2, \tag{16}$$

where $|\mathbf{p}_1|$ and $|\mathbf{p}_2|$ denote the magnitudes of the momentum p_1 and p_2, respectively. In the rest frame of the vector resonance, their expressions are

$$|\mathbf{p}_1| = \frac{1}{2\sqrt{s}}\sqrt{[(m_B^2-m_{P_1}^2)^2]-2(m_B^2+m_{P_1}^2)^2s+s^2},$$
$$|\mathbf{p}_2| = \frac{1}{2\sqrt{s}}\sqrt{[s-(m_{P_2}+m_{P_3})^2][s-(m_{P_2}-m_{P_3})^2]}, \tag{17}$$

where $|\mathbf{p}_2| = q$ in Eq. (6).

III. NUMERICAL RESULTS OF BRANCHING RATIOS

In the numerical calculations, we need input parameters, such as m_V, Γ_0, and $g_{VP_1P_2}$ involved in strong interaction decay of vector mesons, which are listed in the previous section. For the CKM matrix elements needed in the weak transition calculation, we use Wolfenstein parametrization with parameters from the global fit [50] as follows:

$$\lambda = 0.22650 \pm 0.00048, \qquad A = 0.790^{+0.017}_{-0.012},$$
$$\bar\rho = 0.141^{+0.016}_{-0.017}, \qquad \bar\eta = 0.357 \pm 0.01.$$

The decay constants of light pseudoscalar mesons and vector mesons, and transition form factors of B-meson decays at recoil momentum square $Q^2 = 0$ are listed in Tables II and III, respectively. The decay constants of pseudoscalar mesons π, K, and B are from the Particle Data Group [50]. The decay constants of B_s and the vector mesons, and all form factors are not measured by experiments and only calculated theoretically, such as in constitute quark model and light cone quark model [52–55], covariant light front approach [56–58], light-cone sum rules [59–79], PQCD [80–88], and lattice QCD [89–91]. We will use the same theoretical values as in the charmless two-body decays [38], with 5% uncertainty kept for decay constants and 10% for form factors. The dipole model parameters α_1, α_2 applied to describe the Q^2 dependence of form factors are also listed in Table III [54,81].

TABLE III. Transition form factors at $Q^2 = 0$ and dipole model parameters used in this work.

	$F_1^{B\to\pi}$	$F_1^{B\to K}$	$F_1^{B\to\eta_q}$	$A_0^{B\to\rho}$	$A_0^{B\to\omega}$	$A_0^{B\to K^*}$
$F_i(0)$	0.28	0.31	0.21	0.36	0.32	0.39
α_1	0.52	0.54	1.43	1.56	1.60	1.51
α_2	0.45	0.50	0.41	0.17	0.22	0.14

The effective Wilson coefficients $a_i(\mu)$ calculated at next-to-leading order can be found in [92], $a_1(m_b/2) = 1.054$, $a_4(m_b/2) = -0.04$, and $a_9(m_b/2) = -0.009$. The 14 nonpertubative parameters of topological diagrams $\chi^{C^{(\prime)}}, \chi^E, \chi^P, \chi^{P_C^{(\prime)}}, \chi^{P_A}$, and associated phases $\phi^{C^{(\prime)}}, \phi^E, \phi^P, \phi^{P_C^{(\prime)}}, \phi^{P_A}$, extracted from experimental data by a global fit performed in Ref. [38], together with uncertainty are

$$\begin{aligned}
\chi^C &= 0.48 \pm 0.06, & \phi^C &= -1.58 \pm 0.08,\\
\chi^{C'} &= 0.42 \pm 0.16, & \phi^{C'} &= 1.59 \pm 0.17,\\
\chi^E &= 0.057 \pm 0.005, & \phi^E &= 2.71 \pm 0.13,\\
\chi^P &= 0.10 \pm 0.02, & \phi^P &= -0.61 \pm 0.02,\\
\chi^{P_C} &= 0.048 \pm 0.003, & \phi^{P_C} &= 1.56 \pm 0.08,\\
\chi^{P'_C} &= 0.039 \pm 0.003, & \phi^{P'_C} &= 0.68 \pm 0.08,\\
\chi^{P_A} &= 0.0059 \pm 0.0008, & \phi^{P_A} &= 1.51 \pm 0.09.
\end{aligned} \tag{18}$$

With all the inputs, the branching fractions of $B_{(s)} \to P_1V \to P_1P_2P_3$ can be obtained by integrating the differential width in Eq. (16) over the whole kinematics region. Our numerical results for the branching ratios of $B_{(s)}$ decays are collected in Tables IV–VII, for decays $B_{(s)} \to P_1\rho \to P_1\pi\pi$, $B_{(s)} \to P_1K^* \to P_1K\pi$, $B_{(s)} \to P_1\phi \to P_1K\bar K$, and $B_{(s)} \to P_1\rho, P_1\omega \to P_1K\bar K$, respectively. In these tables, we also list the intermediate resonances decays as well as the topological contributions represented by the corresponding symbols T, $C^{(\prime)}$ and so on. In our results, the first uncertainty is from the nonpertubative parameters in Eq. (18), and the other two uncertainties are estimated with 10% variations of form factors, 5% variations of decay constants. One can see that the dominant source of uncertainties are from form factors.

A. Branching ratios of $B_{(s)} \to P_1\rho \to P_1\pi\pi$

Comparing the results shown in Table IV with the corresponding ones calculated in the previous work [38], we find that the branching ratios of quasi-two-body decay $B_{(s)} \to P_1\rho \to P_1\pi\pi$ are a little smaller than that of the direct two-body decays $B_{(s)} \to P_1\rho$. It can be attributed to the not narrow resonance width Γ_ρ. We cannot apply the narrow width approximation to factorize quasi-two-body decay formula together with $\mathcal{B}(\rho \to \pi\pi) \sim 100\%$ to obtain the precise results of two-body decays.

From Table IV, it is easy to see that our results are well consistent with the experimental data shown in the last column of the Table. For the decay modes $B \to \pi(\rho \to)\pi\pi$, $B \to \eta^{(\prime)}(\rho \to)\pi\pi$ with color favored T diagram dominated contribution, and the penguin diagram P dominated modes $B_{(s)} \to K(\rho \to)\pi\pi$, the perturbation calculation is reliable, since these kinds of diagrams are proved to be factorizable to all orders of α_s. Our results are in good agreement with those calculated under the QCD factorization [8] and that in PQCD approach [13] within errors.

For the decay modes with dominated color suppressed diagrams $C^{(\prime)}$ contributions, such as $\bar{B}^0 \to \pi^0(\rho^0 \to)\pi\pi$ and $\bar{B}^0 \to \eta^{(\prime)}(\rho^0 \to)\pi\pi$, the theoretical results are sensitive to the power corrections and next-to-leading order contributions. With the magnitude and phase of this $C^{(\prime)}$ diagram given in Eq. (18), our results of branching ratios are consistent with experimental data and results calculated under the QCD factorization approach [8]. On the contrary, the calculations of these decay modes are only done to the leading order in the perturbative QCD approach with one order magnitude smaller branching ratio [13].

B. Branching ratios of $B_{(s)} \to P_1K^* \to P_1K\pi$

In Table V, we only list quasi-two-body decays $B_{(s)} \to P_1K^* \to P_1K\pi$ through strong decays $K^{*0} \to K^+\pi^-$, $\bar{K}^{*0} \to K^-\pi^+$, and $K^{*-} \to K^-\pi^0$ with a pair of $u\bar{u}$ from the sea. The branching ratios for $B_{(s)} \to P_1K^* \to P_1K\pi$ via sea quark pair $d\bar{d}$ strong decay $K^{*0} \to K^0\pi^0$, $\bar{K}^{*0} \to \bar{K}^0\pi^0$, and $K^{*-} \to \bar{K}^0\pi^-$ can be calculated under the narrow width approximation according to the isospin conservation relationship for strong interaction,

$$\mathcal{B}(\bar{K}^{*0} \to K^-\pi^+) = 2\mathcal{B}(\bar{K}^{*0} \to \bar{K}^0\pi^0), \tag{19}$$

$$\mathcal{B}(K^{*-} \to \bar{K}^0\pi^-) = 2\mathcal{B}(K^{*-} \to K^-\pi^0). \tag{20}$$

The experimental data listed in the last column are measured by *BABAR* [44,94–96] and Belle [97,98] experiments. As we have considered the power corrections from "chiral enhanced" term, penguin annihilation contribution and EW-penguin diagram for the penguin-dominated modes $B_{u,d} \to \pi K^* \to \pi K\pi$, our results are well consistent with experimental data, and larger by a factor of 2–4 than QCD factorization approach [8].

The decay channels $B_{u,d} \to KK^* \to KK\pi$ listed in Table V are CKM suppressed ($|V_{td}/V_{ts}|$) comparing with decay $B_{u,d} \to \pi K^* \to \pi K\pi$, so that the branching ratios of the former are one order magnitude smaller than the latter.

TABLE IV. Branching ratios ($\times 10^{-6}$) of quasi-two-body decays $B_{(s)} \to P_1\rho \to P_1\pi\pi$ together with experimental data [50]. The characters T, $C^{(\prime)}$, E, P, $P_C^{(\prime)}$, P_A, and $P_{\rm EW}$ representing the corresponding topological diagram contributions are also listed in the second column.

Modes	Amplitudes	FAT results	Experiment
$B^- \to \pi^-(\rho^0 \to)\pi^+\pi^-$	$T, C', P, P_A, P_{\rm EW}$	$8.08 \pm 1.74 \pm 1.29 \pm 0.19$	8.30 ± 1.20
$B^- \to \pi^0(\rho^- \to)\pi^-\pi^0$	$T, C, P, P_A, P_{\rm EW}$	$12.70 \pm 0.71 \pm 2.24 \pm 1.12$	10.90 ± 1.40
$\bar{B}^0 \to \pi^-(\rho^+ \to)\pi^+\pi^0$	T, E, P, P_A	$5.72 \pm 0.63 \pm 1.61 \pm 0.33$	8.40 ± 1.10
$\bar{B}^0 \to \pi^+(\rho^- \to)\pi^-\pi^0$	T, E, P	$12.10 \pm 0.91 \pm 3.14 \pm 1.27$	14.60 ± 1.60
$\bar{B}^0 \to \pi^0(\rho^0 \to)\pi^+\pi^-$	$C^{(\prime)}, E, P, P_A, P_{\rm EW}$	$1.23 \pm 0.51 \pm 0.08 \pm 0.16$	2.00 ± 0.50
$B^- \to K^-(\rho^0 \to)\pi^+\pi^-$	$T, C', P, P_{\rm EW}$	$3.41 \pm 0.25 \pm 0.80 \pm 0.04$	3.70 ± 0.50
$B^- \to \bar{K}^0(\rho^- \to)\pi^-\pi^0$	P	$6.85 \pm 0.47 \pm 1.55 \pm 0.07$	$7.30^{+1.00}_{-1.20}$
$\bar{B}^0 \to K^-(\rho^+ \to)\pi^+\pi^0$	$T,\ P$	$7.42 \pm 0.44 \pm 1.65 \pm 0.07$	7.00 ± 0.90
$\bar{B}^0 \to \bar{K}^0(\rho^0 \to)\pi^+\pi^-$	$C', P, P_{\rm EW}$	$4.13 \pm 0.34 \pm 0.79 \pm 0.04$	3.40 ± 1.10
$\bar{B}_s^0 \to K^+(\rho^- \to)\pi^-\pi^0$	T, P, P_A	$17.00 \pm 0 \pm 3.50 \pm 0.20$	⋯
$\bar{B}_s^0 \to K^0(\rho^0 \to)\pi^+\pi^-$	$C', P, P'_C, P_A, P_{\rm EW}$	$1.55 \pm 1.10 \pm 0.31 \pm 0.02$	⋯
$B^- \to \eta(\rho^- \to)\pi^-\pi^0$	$T, C, P, P_C, P_A, P_{\rm EW}$	$7.93 \pm 0.48 \pm 1.43 \pm 0.07$	7.00 ± 2.90
$B^- \to \eta'(\rho^- \to)\pi^-\pi^0$	$T, C, P, P_C, P_A, P_{\rm EW}$	$5.81 \pm 0.48 \pm 1.43 \pm 0.07$	9.70 ± 2.20
$\bar{B}^0 \to \eta(\rho^0 \to)\pi^+\pi^-$	$C^{(\prime)}, E, P, P_C^{(\prime)}, P_A, P_{\rm EW}$	$4.20 \pm 1.15 \pm 0.39 \pm 0.17$	< 1.5
$\bar{B}^0 \to \eta'(\rho^0 \to)\pi^+\pi^-$	$C^{(\prime)}, E, P, P_C^{(\prime)}, P_A, P_{\rm EW}$	$3.09 \pm 0.77 \pm 0.29 \pm 0.12$	< 1.3
$\bar{B}_s^0 \to \eta(\rho^0 \to)\pi^+\pi^-$	$C', E, P'_C, P_{\rm EW}$	$0.11 \pm 0.02 \pm 0.02 \pm 0.003$	⋯
$\bar{B}_s^0 \to \eta'(\rho^0 \to)\pi^+\pi^-$	$C', E, P'_C, P_{\rm EW}$	$0.34 \pm 0.07 \pm 0.05 \pm 0.01$	⋯

TABLE V. Branching ratios ($\times 10^{-6}$) in FAT approach of quasi-two-body decays $B_{(s)} \to P_1 K^* \to P_1 K\pi$, together with experimental data or QCD factorization (QCDF) results. The characters T, $C^{(\prime)}$, E, P, $P_C^{(\prime)}$, P_A, and $P_{\rm EW}$ representing the corresponding topological diagram contributions are also listed in the second column.

Decay modes	Amplitudes	FAT results	Experiment/QCDF
$B^- \to \pi^-(\bar{K}^{*0} \to)K^-\pi^+$	P, P_A	$6.91 \pm 0.66 \pm 1.19 \pm 0.67$	$7.2 \pm 0.4 \pm 0.7^{+0.3}_{-0.5}$[a] $6.45 \pm 0.43 \pm 0.48^{+0.25}_{-0.35}$[b]
$B^- \to \pi^0(K^{*-} \to)K^-\pi^0$	$T, C, P, P_A, P_{\rm EW}$	$1.91 \pm 0.16 \pm 0.29 \pm 0.16$	$2.7 \pm 0.5 \pm 0.4$[a]
$\bar{B}^0 \to \pi^+(K^{*-} \to)K^-\pi^0$	T, P, P_A	$2.57 \pm 0.25 \pm 0.44 \pm 0.25$	$2.7 \pm 0.4 \pm 0.3$[a] $4.9^{+1.5+0.5+0.8}_{-1.5-0.3-0.3}$[b]
$\bar{B}^0 \to \pi^0(\bar{K}^{*0} \to)K^-\pi^+$	$C, P, P_A, P_{\rm EW}$	$2.33 \pm 0.27 \pm 0.44 \pm 0.26$	$2.2 \pm 0.3 \pm 0.3$[a] <2.3[b]
$\bar{B}_s^0 \to \pi^0(K^{*0} \to)K^-\pi^+$	$C, P, P_{\rm EW}$	$0.90 \pm 0.18 \pm 0.17 \pm 0.003$	...
$B^- \to K^-(K^{*0} \to)K^+\pi^-$	P, P_A	$0.40 \pm 0.04 \pm 0.07 \pm 0.04$	$0.22^{+0.00+0.04+0.01}_{-0.00-0.04-0.01}$[c]
$B^- \to K^0(K^{*-} \to)K^-\pi^0$	P	$0.14 \pm 0.01 \pm 0.03 \pm 0.001$	...
$\bar{B}^0 \to K^0(\bar{K}^{*0} \to)K^-\pi^+$	P	$0.27 \pm 0.02 \pm 0.05 \pm 0.002$	...
$\bar{B}^0 \to \bar{K}^0(K^{*0} \to)K^-\pi^+$	P, P_A	$0.37 \pm 0.04 \pm 0.06 \pm 0.04$	$0.20^{+0.00+0.04+0.00}_{-0.00-0.03-0.00}$[c]
$\bar{B}_s^0 \to K^+(K^{*-} \to)K^-\pi^0$	T, E, P, P_A	$2.76 \pm 0.44 \pm 0.31 \pm 0.29$	...
$\bar{B}_s^0 \to K^0(\bar{K}^{*0} \to)K^-\pi^+$	P, P_A	$6.36 \pm 0.98 \pm 0.82 \pm 0.66$	$3.8^{+0.0+0.8+0.0}_{-0.0-0.7-0.0}$[c]
$\bar{B}_s^0 \to \bar{K}^0(K^{*0} \to)K^+\pi^-$	P	$4.28 \pm 0.26 \pm 0.84 \pm 0.04$	$1.5^{+0.0+2.4+0.0}_{-0.0-0.9-0.0}$[c]
$B^- \to \eta(K^{*-} \to)K^-\pi^0$	$T, C, P, P_C, P_A, P_{\rm EW}$	$5.35 \pm 0.37 \pm 0.74 \pm 0.19$	...
$B^- \to \eta'(K^{*-} \to)K^-\pi^0$	$T, C, P, P_C, P_A, P_{\rm EW}$	$1.02 \pm 0.35 \pm 0.12 \pm 0.06$	...
$\bar{B}^0 \to \eta(\bar{K}^{*0} \to)K^-\pi^+$	$C, P, P_C, P_A, P_{\rm EW}$	$11.3 \pm 0.75 \pm 1.53 \pm 0.41$	...
$\bar{B}^0 \to \eta'(\bar{K}^{*0} \to)K^-\pi^+$	$C, P, P_C^{(\prime)}, P_A, P_{\rm EW}$	$2.01 \pm 0.74 \pm 0.21 \pm 0.12$	...
$\bar{B}_s^0 \to \eta(K^{*0} \to)K^+\pi^-$	$C, P, P_C, P_A, P_{\rm EW}$	$0.69 \pm 0.13 \pm 0.11 \pm 0.02$	...
$\bar{B}_s^0 \to \eta'(K^{*0} \to)K^+\pi^-$	$C, P, P_C, P_A, P_{\rm EW}$	$1.17 \pm 0.14 \pm 0.16 \pm 0.04$	...

[a]Experimental data from *BABAR*.
[b]Experimental data from Belle.
[c]Results from QCD factorization approach [8,93].

Since there are not experimental measurements of these decays and $B_s \to KK^* \to KK\pi$, we show in the last column the results of QCD factorization approach [8,93] for comparison. Similarly with the case happened in $B_{u,d} \to \pi K^* \to \pi K\pi$ decays, the results of $B_{u,d} \to KK^* \to KK\pi$ as well as penguin-dominated decays $B_s \to KK^* \to KK\pi$ calculated in the FAT approach are larger by a factor of 2–3 than those in QCD factorization approach [8].

We also give the numerical results of branching ratios of decay modes $B_{(s)} \to \eta K^* \to \eta K\pi$, shown in Table V. These decays have not been measured by experiments from the three-body Dalitz plot analyses. However the corresponding two-body decays have been measured experimentally. Applying the narrow width approximation for the K^* resonance, we have $\Gamma(B_{(s)} \to \eta K^* \to \eta K\pi) = \Gamma(B \to \eta K^*)\mathcal{B}(K^* \to K\pi)$. Utilizing the isospin symmetry relationship

$$\mathcal{B}(K^{*0} \to K^+\pi^-) = \mathcal{B}(K^{*-} \to \bar{K}^0\pi^-) = 2\mathcal{B}(K^{*-} \to K^-\pi^0), \tag{21}$$

we can obtain the branching ratios for two-body decays $B \to \eta K^*$,

$$\mathcal{B}(B^- \to \eta K^{*-}) = (16.05 \pm 1.11 \pm 2.22 \pm 0.57) \times 10^{-6}, \tag{22}$$

$$\mathcal{B}(B^- \to \eta' K^{*-}) = (3.06 \pm 1.05 \pm 0.36 \pm 0.18) \times 10^{-6}, \tag{23}$$

$$\mathcal{B}(\bar{B}^0 \to \eta \bar{K}^{*0}) = (16.95 \pm 1.13 \pm 2.30 \pm 0.62) \times 10^{-6}, \tag{24}$$

$$\mathcal{B}(\bar{B}^0 \to \eta' \bar{K}^{*0}) = (3.02 \pm 1.11 \pm 0.32 \pm 0.18) \times 10^{-6}. \tag{25}$$

These results agree well with the experimental measurements of these two-body decays and the ones given in FAT approach [38].

C. Branching ratios of $B_{(s)} \to P_1\phi \to P_1 K\bar{K}$

We show the branching fraction results of $B_{(s)} \to P_1(\phi \to)K\bar{K}$ decays in Table VI together with the results from PQCD approach [16] in the last column. For penguin

TABLE VI. Branching ratios of quasi-two-body decays $B_{(s)} \to P_1\phi \to P_1 K\bar{K}$ from the FAT approach and that from the PQCD approach. The characters C, P, $P_C^{(\prime)}$, P_A, and $P_{\rm EW}$ representing the corresponding topological diagram contributions are also listed in the second column.

Modes	Amplitudes	$\mathcal{B}_{\rm FAT}$	$\mathcal{B}_{\rm PQCD}$
$B^- \to \pi^-(\phi\to)K^+K^-$	$P'_C, P_{\rm EW}$	$1.47 \pm 0.19 \pm 0.30 \pm 0.15 \times 10^{-7}$	$3.58 \pm 1.17 \pm 1.87 \pm 0.34 \times 10^{-9}$
$\to \pi^-(\phi\to)K^0\bar{K}^0$		$1.03 \pm 0.13 \pm 0.21 \pm 0.10 \times 10^{-7}$	$2.47 \pm 0.81 \pm 1.30 \pm 0.24 \times 10^{-9}$
$\bar{B}^0 \to \pi^0(\phi\to)K^+K^-$	$P'_C, P_{\rm EW}$	$6.82 \pm 0.87 \pm 1.37 \pm 0.68 \times 10^{-8}$	$1.74 \pm 0.53 \pm 0.91 \pm 0.14 \times 10^{-9}$
$\to \pi^0(\phi\to)K^0\bar{K}^0$		$4.78 \pm 0.61 \pm 0.96 \pm 0.48 \times 10^{-8}$	$1.20 \pm 0.37 \pm 0.63 \pm 0.10 \times 10^{-9}$
$\bar{B}_s^0 \to \pi^0(\phi\to)K^+K^-$	$C, P_{\rm EW}$	$1.44 \pm 0.13 \pm 0.29 \pm 0.004 \times 10^{-7}$	$9.11 \pm 2.03 \pm 0.14 \pm 0.61 \times 10^{-8}$
$\to \pi^0(\phi\to)K^0\bar{K}^0$		$1.00 \pm 0.09 \pm 0.20 \pm 0.003 \times 10^{-7}$	$6.30 \pm 1.40 \pm 0.10 \pm 0.43 \times 10^{-8}$
$B^- \to K^-(\phi\to)K^+K^-$	$P, P'_C, P_A, P_{\rm EW}$	$4.53 \pm 1.00 \pm 0.38 \pm 0.52 \times 10^{-6}$	$4.03 \pm 0.67 \pm 0.49 \pm 0.15 \times 10^{-6}$
$\to K^-(\phi\to)K^0\bar{K}^0$		$3.16 \pm 0.70 \pm 0.26 \pm 0.37 \times 10^{-6}$	$2.79 \pm 0.46 \pm 0.34 \pm 0.11 \times 10^{-6}$
$\bar{B}^0 \to \bar{K}^0(\phi\to)K^+K^-$	$P, P'_C, P_A, P_{\rm EW}$	$4.20 \pm 0.93 \pm 0.35 \pm 0.48 \times 10^{-6}$	$3.62 \pm 0.64 \pm 0.59 \pm 0.19 \times 10^{-6}$
$\to \bar{K}^0(\phi\to)K^0\bar{K}^0$		$2.94 \pm 0.65 \pm 0.24 \pm 0.34 \times 10^{-6}$	$2.50 \pm 0.44 \pm 0.41 \pm 0.13 \times 10^{-6}$
$\bar{B}_s^0 \to K^0(\phi\to)K^+K^-$	$P, P'_C, P_{\rm EW}$	$1.84 \pm 0.24 \pm 0.31 \pm 0.035 \times 10^{-7}$	$8.34 \pm 0.48 \pm 0.94 \pm 2.07 \times 10^{-8}$
$\to K^0(\phi\to)K^0\bar{K}^0$		$1.28 \pm 0.16 \pm 0.22 \pm 0.02 \times 10^{-7}$	$5.76 \pm 0.33 \pm 0.65 \pm 1.44 \times 10^{-8}$
$\bar{B}^0 \to \eta(\phi\to)K^+K^-$	$P'_C, P_{\rm EW}$	$4.10 \pm 0.52 \pm 0.82 \pm 0.41 \times 10^{-8}$	…
$\to \eta(\phi\to)K^0\bar{K}^0$		$2.87 \pm 0.37 \pm 0.57 \pm 0.29 \times 10^{-8}$	…
$\bar{B}^0 \to \eta'(\phi\to)K^+K^-$	$P'_C, P_{\rm EW}$	$2.75 \pm 0.35 \pm 0.55 \pm 0.27 \times 10^{-8}$	…
$\to \eta'(\phi\to)K^0\bar{K}^0$		$1.92 \pm 0.25 \pm 0.38 \pm 0.19 \times 10^{-8}$	…
$\bar{B}_s^0 \to \eta(\phi\to)K^+K^-$	$C, P, P_C, P_A, P_{\rm EW}$	$4.14 \pm 2.50 \pm 2.77 \pm 1.21 \times 10^{-7}$	…
$\to \eta(\phi\to)K^0\bar{K}^0$		$2.88 \pm 1.75 \pm 1.92 \pm 0.84 \times 10^{-7}$	…
$\bar{B}_s^0 \to \eta'(\phi\to)K^+K^-$	$C, P, P_C, P_A, P_{\rm EW}$	$6.94 \pm 1.65 \pm 0.52 \pm 0.58 \times 10^{-6}$	…
$\to \eta'(\phi\to)K^0\bar{K}^0$		$4.83 \pm 1.14 \pm 0.36 \pm 0.40 \times 10^{-6}$	…

diagram P dominated decay modes, $B_{u,d} \to K(\phi\to)K\bar{K}$, the results in FAT approach are consistent with the ones in PQCD approach. As discussed in the previous section, this kind of decays are dominated by reliable perturbation contributions, which agree well with the experimental data $\mathcal{B}(B^- \to K^-(\phi\to)K^+K^-) = (4.48 \pm 0.22^{+0.33}_{-0.24}) \times 10^{-6}$ [99] and $\mathcal{B}(B^- \to K^-(\phi\to)K^+K^-) = (4.72 \pm 0.45 \pm 0.35^{+0.39}_{-0.22}) \times 10^{-6}$ [100]. The decay modes $B_s \to K(\phi\to)K\bar{K}$ are CKM suppressed ($|V_{td}/V_{ts}|$) comparing with $B_{u,d} \to K(\phi\to)K\bar{K}$ decays, so that the branching ratios of the former are one order smaller than the latter. It is easy to see from Table VI that branching ratios of all the CKM suppressed decay modes from the FAT approach are larger that that from PQCD approach. It can be attribute to the missing power corrections and next-to-leading order corrections to the color suppressed penguin diagram P'_C in PQCD approach.

Summing over the two quasi-two-body decay modes with same weak decay but different subsequent strong decay, i.e., $B_{(s)} \to P_1(\phi\to)K^+K^-$ and $B_{(s)} \to P_1(\phi\to)K^0\bar{K}^0$, we should obtain results of the corresponding two-body decays $B_{(s)} \to P_1\phi$ by applying the narrow width approximation. For instance, the summation of the results of $\mathcal{B}(B^- \to \pi^-(\phi\to)K^+K^-)$ and $\mathcal{B}(B^- \to \pi^-(\phi\to)K^0\bar{K}^0)$ in Table VI is in agreement with the two-body decay value $\mathcal{B}(B^- \to \pi^-\phi) = (2.80 \pm 0.04 \pm 0.55 \pm 0.03) \times 10^{-7}$ in [38] within the error bar.

D. The virtual effects of $B_{(s)} \to \pi,K(\rho,\omega\to)K\bar{K}$

The decay modes $B_{(s)} \to \pi, K(\rho,\omega\to)K\bar{K}$ represent a category of decays, whose pole masses of the resonances ρ, ω smaller than the threshold mass of producing $K\bar{K}$ pair. They can only happen with the virtual effect, which is also called the Breit-Wigner tail effect. In Table VII, we collect these virtual effects in the FAT approach, together with the results in PQCD approach [17] for comparison. Here we only show subprocesses $\rho^0,\omega \to K^+K^-$ without $\rho^0,\omega \to K^0\bar{K}^0$ due to the tiny mass difference between K^+K^- and $K^0\bar{K}^0$. The virtual effects of $B_{(s)} \to \pi, K(\rho\to)K\bar{K}$ are approximately 1–2 order smaller than the dominated contribution of $B_{(s)} \to \pi, K(\rho\to)\pi\pi$ in Table IV. Unlike the on-shell resonance contributions that mostly give the similar contributions between the FAT and PQCD approaches, the virtual contributions give quite different results between the two approaches. Since the color suppressed tree diagram $C^{(\prime)}$ is calculated in PQCD approach only to the leading order, its size is significantly smaller that that fitted from experimental data in FAT approach [38]. As a result, the off-shell effects in $C^{(\prime)}$ dominated decay modes, $\bar{B}^0 \to \pi^0(\rho^0,\omega\to)K^+K^-$, $\bar{B}_s^0 \to K^0(\rho^0,\omega\to)K^+K^-$ using the FAT approach are nearly one order magnitude larger than that of PQCD approach. For another example, the hierarchy between the magnitude of virtual contributions for quasi-two-body decays $B^- \to \pi^0(\rho^-\to)K^-K^0$ and $B^- \to \pi^-(\rho^0\to)K^+K^-$ is opposite in the PQCD and FAT

TABLE VII. Comparison of results from the FAT and PQCD approaches for the virtual effects of $B_{(s)} \to \pi, K(\rho, \omega \to)K\bar{K}$ decays, which happened when the pole masses of ρ, ω are smaller than the invariant mass of $K\bar{K}$.

Modes	$\mathcal{B}_{\mathrm{FAT}}$	$\mathcal{B}_{\mathrm{PQCD}}$
$B^- \to \pi^0(\rho^- \to)K^-K^0$	$1.02 \pm 0.05 \pm 0.19 \pm 0.09 \times 10^{-7}$	$2.01^{+0.38+0.29+0.24+0.10+0.06}_{-0.35-0.26-0.20-0.07-0.06} \times 10^{-8}$
$B^- \to \pi^-(\rho^0 \to)K^+K^-$	$5.48 \pm 1.40 \pm 0.85 \pm 0.16 \times 10^{-8}$	$1.43^{+0.26+0.19+0.11+0.06+0.04}_{-0.25-0.17-0.10-0.05-0.04} \times 10^{-7}$
$B^- \to \pi^-(\omega \to)K^+K^-$	$4.48 \pm 1.15 \pm 0.70 \pm 0.13 \times 10^{-8}$	$4.21^{+1.67+1.03+0.08+0.21+0.14}_{-1.34-0.96-0.08-0.17-0.14} \times 10^{-8}$
$\bar{B}^0 \to \pi^+(\rho^- \to)K^-K^0$	$1.10 \pm 0.07 \pm 0.27 \pm 0.11 \times 10^{-7}$	$1.02^{+0.21+0.28+0.14+0.06+0.03}_{-0.17-0.25-0.13-0.05-0.03} \times 10^{-7}$
$\bar{B}^0 \to \pi^-(\rho^+ \to)K^+\bar{K}^0$	$3.51 \pm 0.39 \pm 0.99 \pm 0.20 \times 10^{-8}$	$9.59^{+3.25+1.96+0.22+0.46+0.29}_{-2.90-1.88-0.19-0.33-0.29} \times 10^{-8}$
$\bar{B}^0 \to \pi^0(\rho^0 \to)K^+K^-$	$7.54 \pm 3.39 \pm 0.44 \pm 1.03 \times 10^{-9}$	$1.47^{+0.96+0.53+0.19+0.13+0.04}_{-0.78-0.49-0.14-0.07-0.04} \times 10^{-9}$
$\bar{B}^0 \to \pi^0(\omega \to)K^+K^-$	$1.60 \pm 0.67 \pm 0.18 \pm 0.11 \times 10^{-8}$	$4.96^{+0.73+1.25+0.63+0.24+0.17}_{-0.87-1.36-0.65-0.22-0.17} \times 10^{-9}$
$B^- \to \bar{K}^0(\rho^- \to)K^-K^0$	$4.16 \pm 0.25 \pm 0.84 \pm 0.04 \times 10^{-8}$	$2.21^{+0.51+0.51+0.34+0.10+0.07}_{-0.45-0.46-0.29-0.08-0.07} \times 10^{-7}$
$B^- \to K^-(\rho^0 \to)K^+K^-$	$2.13 \pm 0.14 \pm 0.43 \pm 0.02 \times 10^{-8}$	$5.15^{+0.91+0.99+0.69+0.25+0.16}_{-0.85-0.98-0.66-0.21-0.16} \times 10^{-8}$
$B^- \to K^-(\omega \to)K^+K^-$	$5.09 \pm 0.84 \pm 0.95 \pm 0.47 \times 10^{-8}$	$8.92^{+1.67+2.33+1.19+0.43+0.30}_{-1.47-2.18-1.07-0.34-0.30} \times 10^{-8}$
$\bar{B}^0 \to K^-(\rho^+ \to)K^+\bar{K}^0$	$4.51 \pm 0.24 \pm 0.91 \pm 0.04 \times 10^{-8}$	$1.77^{+0.30+0.41+0.27+0.08+0.05}_{-0.25-0.39-0.25-0.06-0.05} \times 10^{-7}$
$\bar{B}^0 \to \bar{K}^0(\rho^0 \to)K^+K^-$	$2.71 \pm 0.24 \pm 0.45 \pm 0.06 \times 10^{-8}$	$5.44^{+0.88+1.26+0.82+0.24+0.17}_{-0.81-1.19-0.76-0.18-0.17} \times 10^{-8}$
$\bar{B}^0 \to \bar{K}^0(\omega \to)K^+K^-$	$3.81 \pm 0.71 \pm 0.81 \pm 0.41 \times 10^{-8}$	$5.99^{+1.15+1.60+0.88+0.22+0.20}_{-0.96-1.39-0.75-0.19-0.20} \times 10^{-8}$
$\bar{B}_s^0 \to K^+(\rho^- \to)K^-K^0$	$1.40 \pm 0.003 \pm 0.28 \pm 0.14 \times 10^{-7}$	$2.04^{+0.03+0.43+0.22+0.11+0.06}_{-0.02-0.41-0.21-0.09-0.06} \times 10^{-7}$
$\bar{B}_s^0 \to K^0(\rho^0 \to)K^+K^-$	$1.29 \pm 0.90 \pm 0.25 \pm 0.13 \times 10^{-8}$	$1.03^{+0.63+0.19+0.18+0.08+0.03}_{-0.45-0.17-0.16-0.05-0.03} \times 10^{-9}$
$\bar{B}_s^0 \to K^0(\omega \to)K^+K^-$	$1.09 \pm 0.72 \pm 0.20 \pm 0.11 \times 10^{-8}$	$1.39^{+0.68+0.17+0.12+0.07+0.05}_{-0.57-0.14-0.14-0.07-0.05} \times 10^{-9}$

approaches, which need further experimental measurements to check.

Comparing the results between Tables IV and VII, one can see that the off-shell effects in $B \to \pi, K(\rho \to)K\bar{K}$ are small, that is only about 1% of the on-resonance contribution. However from Table VII, one can see that the off-shell effect from the ground state $\rho(770)^0$ in $B^- \to \pi^-(\rho^0 \to)K^+K^-$ decay in FAT approach is at the same order as the branching ratio

$$\mathcal{B}(B^- \to \pi^-(\rho(1450)^0 \to)K^+K^-) = (9.46^{+1.79+1.16+0.72+0.49+1.82}_{-1.65-1.14-0.69-0.38-1.82}) \times 10^{-8}, \quad (26)$$

calculated by PQCD approach [17]. The latter branching fraction of $B^- \to \pi^-(\rho(1450)^0 \to)K^+K^-$ was measured by LHCb [101], Belle [102], and *BABAR* [103]. Therefore the virtual contribution of $B^- \to \pi^-(\rho(770)^0 \to)K^+K^-$ should also be considered in experimental analysis.

Comparing the virtual effect contributions of ρ with ω resonance in Table VII, for instance, $B^- \to \pi^-(\rho^0 \to)K^+K^-$ and $B^- \to \pi^-(\omega \to)K^+K^-$, we find that the virtual effects are at the same order magnitude, even though the decay widths of ρ and ω meson are very different, shown in Table I. It means that the virtual contributions of these decays are not very sensitive to the full decay width of ρ and ω meson, which is also confirmed by the PQCD approach [17]. This can be explained by the behavior of the Breit-Wigner propagators in Eq. (5) in the kinematics regions of these decays, where the imaginary part $im_{\rho,\omega}\Gamma_{\rho,\omega}(s)$ becomes unimportant when the invariant mass square s is larger than 1 GeV^2.

IV. *CP* ASYMMETRY

The study of three-body B decays attracts a lot of interests because of its large CP asymmetry. In this work, we will concentrate on direct CP violation and will not discuss mixing-induced CP violation. We also do not consider integrated CP asymmetry of the whole phase space of three-body B decays, but we only consider the direct CP asymmetry of quasi-two-body decay with one resonant as the intermediate state. Consequently this CP asymmetry will arise from the interference between tree and penguin amplitudes of the two-body resonances but not from the interference between three-body nonresonant and resonant contribution or between different resonant states.

It is well known that direct CP asymmetries are induced by the interference between difference of strong phases and different CKM phases of different contributions. The strong phase is also the major source of direct CP violation uncertainty as it is mostly from nonperturbative QCD dynamics. As illustrated in Ref. [38] for the two-body B decays, the strong phases extracted from experimental data are sufficient to induce correct direct CP asymmetry, while QCD factorization approaches and soft-collinear effect theory usually make wrong predictions or no prediction for the direct CP asymmetries due to absence of nonperturbative strong phases, such as the well-known $K\pi$ puzzle. The problem in two-body decays will also exist in three-body decays. For example, the signs of CP asymmetry of $B^- \to \pi^-K^+K^-$ and $B^- \to K^-\pi^+\pi^-$ decay were in conflict with experimental data under the QCD factorization approach [8]. The authors need to consider the final-state rescattering effect by introducing an unknown strong

TABLE VIII. Direct CP asymmetry of quasi-two-body decay $B_{(s)} \to P_1\rho \to P_1\pi\pi$ together with experimental data [50].

Modes	Amplitudes	Quasi-two-body results	Experiment
$B^- \to \pi^-(\rho^0 \to)\pi^+\pi^-$	$T, C', P, P_A, P_{\rm EW}$	-0.43 ± 0.04	0.009 ± 0.019
$B^- \to \pi^0(\rho^- \to)\pi^-\pi^0$	$T, C, P, P_A, P_{\rm EW}$	0.15 ± 0.02	0.02 ± 0.11
$\bar{B}^0 \to \pi^-(\rho^+ \to)\pi^+\pi^0$	T, E, P, P_A	-0.43 ± 0.03	-0.08 ± 0.08
$\bar{B}^0 \to \pi^+(\rho^- \to)\pi^+\pi^0$	T, E, P	0.14 ± 0.03	0.13 ± 0.06
$\bar{B}^0 \to \pi^0(\rho^0 \to)\pi^+\pi^-$	$C^{(\prime)}, E, P, P_A, P_{\rm EW}$	0.34 ± 0.08	-0.27 ± 0.24
$B^- \to K^-(\rho^0 \to)\pi^+\pi^-$	$T, C', P, P_{\rm EW}$	0.62 ± 0.06	0.37 ± 0.10
$B^- \to \bar{K}^0(\rho^- \to)\pi^+\pi^0$	P	0.009 ± 0.000	-0.03 ± 0.15
$\bar{B}^0 \to K^-(\rho^+ \to)\pi^-\pi^0$	T, P	0.59 ± 0.01	0.21 ± 0.11
$\bar{B}^0 \to \bar{K}^0(\rho^0 \to)\pi^+\pi^-$	$C', P, P_{\rm EW}$	-0.085 ± 0.059	-0.06 ± 0.09
$\bar{B}_s^0 \to K^+(\rho^- \to)\pi^+\pi^0$	T, P, P_A	0.15 ± 0.03	…
$\bar{B}_s^0 \to K^0(\rho^0 \to)\pi^+\pi^-$	$C', P, P'_C, P_A, P_{\rm EW}$	-0.40 ± 0.14	…
$B^- \to \eta(\rho^- \to)\pi^+\pi^0$	$T, C, P, P_C, P_A, P_{\rm EW}$	-0.11 ± 0.02	0.11 ± 0.11
$B^- \to \eta'(\rho^- \to)\pi^+\pi^0$	$T, C, P, P_C, P_A, P_{\rm EW}$	0.42 ± 0.05	0.26 ± 0.17
$\bar{B}^0 \to \eta(\rho^0 \to)\pi^+\pi^-$	$C^{(\prime)}, E, P, P_C^{(\prime)}, P_A, P_{\rm EW}$	-0.22 ± 0.03	-0.23 ± 0.03
$\bar{B}^0 \to \eta'(\rho^0 \to)\pi^+\pi^-$	$C^{(\prime)}, E, P, P_C^{(\prime)}, P_A, P_{\rm EW}$	0.083 ± 0.078	…
$\bar{B}_s^0 \to \eta(\rho^0 \to)\pi^+\pi^-$	$C', E, P'_C, P_{\rm EW}$	-0.50 ± 0.39	…
$\bar{B}_s^0 \to \eta'(\rho^0 \to)\pi^+\pi^-$	$C', E, P'_C, P_{\rm EW}$	-0.64 ± 0.09	…

phase δ to account for the sign flip of CP asymmetry. Therefore possible $1/m_b$ power corrections, such as final-state interactions, or other nonperturbative contributions are necessary to correctly describe CP asymmetry. For the quasi-two-body decays under the framework of FAT, the strong phases result in from the nonperturbative contribution parameters in Eq. (18) and the Breit-Wigner formalism for resonance in Eq. (5). These strong phases have already contained all perturbative and nonperturbative QCD effects, for instance, final-state interactions, color suppressed contribution, penguin annihilation contribution, and so on. They explain well the measured branching ratios and thus are expected to give the right prediction of CP asymmetry parameters in three-body B decays.

We show the CP asymmetries of $B_{(s)} \to P_1\rho \to P_1\pi\pi$ and $B_{(s)} \to P_1K^* \to P_1K\pi$ in Tables VIII and IX,

TABLE IX. The same as Table VIII, but for the quasi-two-body of quasi-two-body decays $B_{(s)} \to P_1K^* \to P_1K\pi$.

Modes	Amplitudes	Quasi-two-body results	Experiment
$B^- \to \pi^-(\bar{K}^{*0} \to)K^-\pi^+$	P, P_A	0.006 ± 0.001	-0.04 ± 0.09
$B^- \to \pi^0(K^{*-} \to)K^-\pi^0$	$T, C, P, P_A, P_{\rm EW}$	0.09 ± 0.04	-0.39 ± 0.21
$\bar{B}^0 \to \pi^+(K^{*-} \to)K^-\pi^0$	T, P, P_A	-0.21 ± 0.04	-0.27 ± 0.04
$\bar{B}^0 \to \pi^0(\bar{K}^{*0} \to)K^-\pi^+$	$C, P, P_A, P_{\rm EW}$	-0.27 ± 0.05	-0.15 ± 0.13
$\bar{B}_s^0 \to \pi^0(K^{*0} \to)K^-\pi^+$	$C, P, P_{\rm EW}$	-0.29 ± 0.06	…
$B^- \to K^-(K^{*0} \to)K^+\pi^-$	P, P_A	-0.11 ± 0.02	0.12 ± 0.10
$B^- \to K^0(K^{*-} \to)K^-\pi^0$	P	-0.19 ± 0.18	…
$\bar{B}^0 \to K^0(\bar{K}^{*0} \to)K^-\pi^+$	P	-0.19 ± 0.01	…
$\bar{B}^0 \to \bar{K}^0(K^{*0} \to)K^-\pi^+$	P, P_A	-0.11 ± 0.02	…
$\bar{B}_s^0 \to K^+(K^{*-} \to)K^-\pi^0$	T, E, P, P_A	-0.31 ± 0.04	…
$\bar{B}_s^0 \to K^0(\bar{K}^{*0} \to)K^-\pi^+$	P, P_A	0.002 ± 0.001	…
$\bar{B}_s^0 \to \bar{K}^0(K^{*0} \to)K^+\pi^-$	P	0.009 ± 0.000	…
$B^- \to \eta(K^{*-} \to)K^-\pi^0$	$T, C, P, P_C, P_A, P_{\rm EW}$	-0.18 ± 0.02	0.02 ± 0.06
$B^- \to \eta'(K^{*-} \to)K^-\pi^0$	$T, C, P, P_C, P_A, P_{\rm EW}$	-0.47 ± 0.09	-0.26 ± 0.27
$\bar{B}^0 \to \eta(\bar{K}^{*0} \to)K^-\pi^+$	$C, P, P_C, P_A, P_{\rm EW}$	0.067 ± 0.012	0.19 ± 0.05
$\bar{B}^0 \to \eta'(\bar{K}^{*0} \to)K^-\pi^+$	$C, P, P_C^{(\prime)}, P_A, P_{\rm EW}$	0.062 ± 0.052	-0.07 ± 0.18
$\bar{B}_s^0 \to \eta(K^{*0} \to)K^+\pi^-$	$C, P, P_C, P_A, P_{\rm EW}$	0.58 ± 0.12	…
$\bar{B}_s^0 \to \eta'(K^{*0} \to)K^+\pi^-$	$C, P, P_C, P_A, P_{\rm EW}$	-0.45 ± 0.10	…

respectively. As the theoretical uncertainty from hadronic parameters (form factors and decay constants) mostly cancel, the major theoretical uncertainties for CP asymmetry parameters are from the nonperturbative contribution parameters in Eq. (18) and weak phases. Here we only list the uncertainty arise from the strong phase in Eq. (18) due to small uncertainties of CKM matrix elements. We also list the experimental data in the last column of the two tables. Actually only three decay modes with the intermediate process $K^-\rho^0$, π^+K^{*-}, and $\eta\bar{K}^{*0}$ are well measured in experiments with more than 3σ signal significance. Most CP asymmetries listed here are predictions to be tested by the future experiments. For example, the CP asymmetry of $B^- \to \pi^+\rho^0 \to \pi^+\pi^+\pi^-$ is predicted quite large in this work, which is consistent with the theoretical predictions using QCDF [30] and the PQCD approach [13] but not yet measured by the experiments. We did not list the CP asymmetries of $B \to P_1\phi \to P_1K\bar{K}$ decays in our table, since most of them are from pure penguin diagram contributions, P_C, P_A, whose CP asymmetry is expected to be zero with only one single CKM phase, at leading order approximation. We also do not list the CP asymmetries of $B_{(s)} \to P_1\rho(\omega) \to P_1K\bar{K}$ decays contributed by the virtual effects.

Most of the quasi-two-body decays are extracted from the Dalitz-plot analysis of three-body ones in experimental analysis. For example, $B^- \to K^-\rho^0$ and $B^- \to \pi^-\bar{K}^{*0}$ decays are extracted from $B^- \to K^-\pi^+\pi^-$ decays. Comparing the CP asymmetries of quasi-two-body decay by integrating out the invariant mass square (s) distribution of CP asymmetry over the kinematics region in the Dalitz plot with the corresponding ones of two-body decay with s fixed as m_V^2 as in Ref. [38], we find that the size of CP asymmetries of $B_{(s)} \to P_1\rho \to P_1\pi\pi$ in Table VIII are slightly smaller than that of $B_{(s)} \to P_1\rho$. The CP asymmetry of $B_{(s)} \to P_1K^* \to P_1K\pi$ in Table IX are slightly larger than that of the $B_{(s)} \to P_1K^*$ decay. These very small changes of CP asymmetry between two-body and quasi-two-body decays arise from the finite decay width of vector resonances.

V. CONCLUSION

We systematically analyze the three-body charmless B meson decays through the intermediate resonance, i.e., they proceed via quasi-two-body decays as $B_{(s)} \to P_1V \to P_1P_2P_3$, with the vector resonant state V including all ground states ρ, K^*, ω, ϕ. The first step of two-body B decays to P_1V intermediate states is induced by flavor changing weak decays $b \to u\bar{u}d(s)$ at leading order and $b \to d(s)q\bar{q}(q = u, d, s)$ at one loop level. The second step is that the intermediate vector resonant state V, described by the Breit-Wigner propagator, decays into two light pseudoscalar mesons via strong interaction. In order to include all possible perturbative and nonperturbative QCD corrections, the two-body weak B decays are described by the FAT approach with the decay amplitudes extracted from experimental data.

We compare results of the branching fractions from FAT approach with the PQCD approach's predictions and the ones of QCD factorization, as well as the experimental data. For a color suppressed tree diagram and color suppressed or annihilation penguin diagram dominated decay modes, the branching ratios in FAT approach are larger than that of the PQCD approach and the QCD factorization approach. The reason is that the decay magnitudes and phases extracted from experimental data in FAT approach are larger than that in the other two approaches due to the shortage of nonperturbative contribution and $1/m_b$ power corrections. We have also considered the virtual effects from ρ and ω resonance tail, which are usually ignored by the experimental analysis. These virtual effects from ground state $\rho(770)^0$ are about 1–2 order magnitude smaller than the dominated contribution of $B_{(s)} \to \pi, K(\rho \to)\pi\pi$ decays. However, these virtual effects contributions are at the same order as the higher resonance contributions, such as $\rho(1450)$. We also find that the virtual contributions of these decays are not very sensitive to the decay widths of ρ and ω. The branching ratios of $B_{(s)} \to P_1(\rho \to)\pi\pi$, $B_{(s)} \to P_1(K^* \to)K\pi$ are consistent with experimental data, and the others are predictions waiting for future experiments to test.

For CP asymmetry, theoretical predictions of three-body decays are mostly based on quasi-two-body decays via intermediate resonance, where the strong phases extracted from experimental data in FAT approach are sufficient to induce correct direct CP asymmetries. In this work, we utilize the same strong phases of two-body decays together with the phases from Breit-Wigner formalism to predict the direct CP asymmetries of quasi-two-body decays, $B_{(s)} \to P_1(\rho \to)\pi\pi$ and $B_{(s)} \to P_1(K^* \to)K\pi$. Our results agree well with the existing experimental measurements. But many of the CP asymmetry predictions are waiting for future experiments.

ACKNOWLEDGMENTS

S.-H. Z. thanks Theoretical Physics Division of Institute of High Energy Physics, CAS for hospitality while this work was completed. The work is supported by the National Natural Science Foundation of China under Grants No. 11765012, No. 12075126, No. 12275277, No. 12070131001, and No. 12105148, as well as the National Key Research and Development Program of China under Contract No. 2020YFA0406400.

[1] B. Aubert *et al.* (*BABAR* Collaboration), Dalitz plot analysis of $B^{\pm} \to \pi^{\pm}\pi^{\pm}\pi^{\mp}$ decays, Phys. Rev. D **79**, 072006 (2009).

[2] I. Nasteva, Studies of charmless B decays including *CP* violation effects, in *Proceedings of the 11th Conference on Flavor Physics and CP Violation* (2013), arXiv:1308.0740.

[3] R. Aaij *et al.* (LHCb Collaboration), Measurement of *CP* Violation in the Phase Space of $B^{\pm} \to K^{+}K^{-}\pi^{\pm}$ and $B^{\pm} \to \pi^{+}\pi^{-}\pi^{\pm}$ Decays, Phys. Rev. Lett. **112**, 011801 (2014).

[4] R. Aaij *et al.* (LHCb Collaboration), Measurements of *CP* violation in the three-body phase space of charmless $B^{\pm}$ decays, Phys. Rev. D **90**, 112004 (2014).

[5] J. P. Lees *et al.* (*BABAR* Collaboration), Evidence for *CP* violation in $B^{+} \to K^{*}(892)^{+}\pi^{0}$ from a Dalitz plot analysis of $B^{+} \to K^{0}_{S}\pi^{+}\pi^{0}$ decays, Phys. Rev. D **96**, 072001 (2017).

[6] H.-Y. Cheng and K.-C. Yang, Nonresonant three-body decays of D and B mesons, Phys. Rev. D **66**, 054015 (2002).

[7] H.-Y. Cheng, C.-K. Chua, and A. Soni, Charmless three-body decays of B mesons, Phys. Rev. D **76**, 094006 (2007).

[8] H.-Y. Cheng and C.-K. Chua, Branching fractions and direct *CP* violation in charmless three-body decays of B mesons, Phys. Rev. D **88**, 114014 (2013).

[9] S. Kränkl, T. Mannel, and J. Virto, Three-body nonleptonic B decays and QCD factorization, Nucl. Phys. **B899**, 247 (2015).

[10] C.-H. Chen and H.-n. Li, Three body nonleptonic B decays in perturbative QCD, Phys. Lett. B **561**, 258 (2003).

[11] W.-F. Wang, H.-C. Hu, H.-n. Li, and C.-D. Lü, Direct *CP* asymmetries of three-body B decays in perturbative QCD, Phys. Rev. D **89**, 074031 (2014).

[12] W.-F. Wang and H.-n. Li, Quasi-two-body decays $B \to K\rho \to K\pi\pi$ in perturbative QCD approach, Phys. Lett. B **763**, 29 (2016).

[13] Y. Li, A.-J. Ma, W.-F. Wang, and Z.-J. Xiao, Quasi-two-body decays $B_{(s)} \to P\rho \to P\pi\pi$ in perturbative QCD approach, Phys. Rev. D **95**, 056008 (2017).

[14] Y. Li, W.-F. Wang, A.-J. Ma, and Z.-J. Xiao, Quasi-two-body decays $B_{(s)} \to K^{*}(892)h \to K\pi h$ in perturbative QCD approach, Eur. Phys. J. C **79**, 37 (2019).

[15] W.-F. Wang, Will the subprocesses $\rho(770, 1450)^{0} \to K^{+}K^{-}$ contribute large branching fractions for $B^{\pm} \to \pi^{\pm}K^{+}K^{-}$ decays?, Phys. Rev. D **101**, 111901(R) (2020).

[16] Y.-Y. Fan and W.-F. Wang, Resonance contributions $\phi(1020, 1680) \to K\bar{K}$ for the three-body decays $B \to K\bar{K}h$, Eur. Phys. J. C **80**, 815 (2020).

[17] W.-F. Wang, Contributions for the kaon pair from $\rho(770)$, $\omega(782)$ and their excited states in the $B \to K\bar{K}h$ decays, Phys. Rev. D **103**, 056021 (2021).

[18] Z.-T. Zou, Y. Li, Q.-X. Li, and X. Liu, Resonant contributions to three-body $B \to KKK$ decays in perturbative QCD approach, Eur. Phys. J. C **80**, 394 (2020).

[19] Z.-T. Zou, Y. Li, and X. Liu, Branching fractions and *CP* asymmetries of the quasi-two-body decays in $B_s \to K^{0}(\bar{K}^{0})K^{\pm}\pi^{\mp}$ within PQCD approach, Eur. Phys. J. C **80**, 517 (2020).

[20] Z.-T. Zou, L. Yang, Y. Li, and X. Liu, Study of quasi-two-body $B_{(s)} \to \phi(f_0(980)/f_2(1270) \to)\pi\pi$ decays in perturbative QCD approach, Eur. Phys. J. C **81**, 91 (2021).

[21] L. Yang, Z.-T. Zou, Y. Li, X. Liu, and C.-H. Li, Quasi-two-body $B_{(s)} \to V\pi\pi$ decays with resonance $f_0(980)$ in the PQCD approach, Phys. Rev. D **103**, 113005 (2021).

[22] W.-F. Liu, Z.-T. Zou, and Y. Li, Charmless quasi-two-body B decays in perturbative QCD approach: Taking $B \to K(R \to)K^{+}K^{-}$ as examples, Adv. High Energy Phys. **2022**, 5287693 (2022).

[23] R. Klein, T. Mannel, J. Virto, and K. K. Vos, *CP* violation in multibody B decays from QCD factorization, J. High Energy Phys. 10 (2017) 117.

[24] T. Mannel, K. Olschewsky, and K. K. Vos, *CP* violation in three-body B decays: A model ansatz, J. High Energy Phys. 06 (2020) 073.

[25] S. Cheng, A. Khodjamirian, and J. Virto, $B \to \pi\pi$ form factors from light-cone sum rules with B-meson distribution amplitudes, J. High Energy Phys. 05 (2017) 157.

[26] S. Descotes-Genon, A. Khodjamirian, and J. Virto, Light-cone sum rules for $B \to K\pi$ form factors and applications to rare decays, J. High Energy Phys. 12 (2019) 083.

[27] C. Hambrock and A. Khodjamirian, Form factors in $\bar{B}^{0} \to \pi\pi\ell\bar{\nu}_{\ell}$ from QCD light-cone sum rules, Nucl. Phys. **B905**, 373 (2016).

[28] S. Cheng, A. Khodjamirian, and J. Virto, Timelike-helicity $B \to \pi\pi$ form factor from light-cone sum rules with dipion distribution amplitudes, Phys. Rev. D **96**, 051901 (2017).

[29] T. Huber, J. Virto, and K. K. Vos, Three-body non-leptonic heavy-to-heavy B decays at NNLO in QCD, J. High Energy Phys. 11 (2020) 103.

[30] H.-Y. Cheng and C.-K. Chua, Revisiting Charmless Hadronic $B_{u,d}$ decays in QCD factorization, Phys. Rev. D **80**, 114008 (2009).

[31] J. Chai, S. Cheng, Y.-h. Ju, D.-C. Yan, C.-D. Lü, and Z.-J. Xiao, Charmless two-body B meson decays in the perturbative QCD factorization approach, Chin. Phys. C **46**, 123103 (2022).

[32] H.-Y. Cheng, C.-W. Chiang, and A.-L. Kuo, Updating $B \to PP, VP$ decays in the framework of flavor symmetry, Phys. Rev. D **91**, 014011 (2015).

[33] X.-G. He, Y.-J. Shi, and W. Wang, Unification of flavor SU(3) analyses of heavy hadron weak decays, Eur. Phys. J. C **80**, 359 (2020).

[34] X.-G. He and W. Wang, Flavor SU(3) topological diagram and irreducible representation amplitudes for heavy meson charmless hadronic decays: Mismatch and equivalence, Chin. Phys. C **42**, 103108 (2018).

[35] H.-n. Li, C.-D. Lu, and F.-S. Yu, Branching ratios and direct *CP* asymmetries in $D \to PP$ decays, Phys. Rev. D **86**, 036012 (2012).

[36] Q. Qin, H.-n. Li, C.-D. Lü, and F.-S. Yu, Branching ratios and direct *CP* asymmetries in $D \to PV$ decays, Phys. Rev. D **89**, 054006 (2014).

[37] S.-H. Zhou, Y.-B. Wei, Q. Qin, Y. Li, F.-S. Yu, and C.-D. Lu, Analysis of two-body charmed B meson decays in factorization-assisted topological-amplitude approach, Phys. Rev. D **92**, 094016 (2015).

[38] S.-H. Zhou, Q.-A. Zhang, W.-R. Lyu, and C.-D. Lü, Analysis of charmless two-body B decays in factorization

assisted topological amplitude approach, Eur. Phys. J. C **77**, 125 (2017).
[39] H.-Y. Jiang, F.-S. Yu, Q. Qin, H.-n. Li, and C.-D. Lü, $D^0 - \bar{D}^0$ mixing parameter y in the factorization-assisted topological-amplitude approach, Chin. Phys. C **42**, 063101 (2018).
[40] S.-H. Zhou and C.-D. Lü, Extraction of the CKM phase γ from the charmless two-body B meson decays, Chin. Phys. C **44**, 063101 (2020).
[41] S.-H. Zhou, R.-H. Li, Z.-Y. Wei, and C.-D. Lu, Analysis of three-body charmed B-meson decays under the factorization-assisted topological-amplitude approach, Phys. Rev. D **104**, 116012 (2021).
[42] Q. Qin, C. Wang, D. Wang, and S.-H. Zhou, The factorization-assisted topological-amplitude approach and its applications, arXiv:2111.14472.
[43] C. W. Bauer, S. Fleming, D. Pirjol, and I. W. Stewart, An effective field theory for collinear and soft gluons: Heavy to light decays, Phys. Rev. D **63**, 114020 (2001).
[44] J. P. Lees *et al.* (*BABAR* Collaboration), Amplitude analysis of $B^0 \to K^+\pi^-\pi^0$ and evidence of direct CP violation in $B \to K^*\pi$ decays, Phys. Rev. D **83**, 112010 (2011).
[45] J. P. Lees *et al.* (*BABAR* Collaboration), Precise measurement of the $e^+e^- \to \pi^+\pi^-(\gamma)$ cross section with the initial-state radiation method at *BABAR*, Phys. Rev. D **86**, 032013 (2012).
[46] R. Aaij *et al.* (LHCb Collaboration), Amplitude analysis of the $B^+ \to \pi^+\pi^+\pi^-$ decay, Phys. Rev. D **101**, 012006 (2020).
[47] J. M. Blatt and V. F. Weisskopf, *Theoretical Nuclear Physics* (Springer, New York, 1952).
[48] R. Aaij *et al.* (LHCb Collaboration), Dalitz plot analysis of $B_s^0 \to \bar{D}^0 K^-\pi^+$ decays, Phys. Rev. D **90**, 072003 (2014).
[49] R. Aaij *et al.* (LHCb Collaboration), Amplitude analysis of $B^- \to D^+\pi^-\pi^-$ decays, Phys. Rev. D **94**, 072001 (2016).
[50] R. L. Workman *et al.* (Particle Data Group), Review of particle physics, Prog. Theor. Exp. Phys. **2022**, 083C01 (2022).
[51] C. Bruch, A. Khodjamirian, and J. H. Kuhn, Modeling the pion and kaon form factors in the timelike region, Eur. Phys. J. C **39**, 41 (2005).
[52] D. Melikhov and B. Stech, Weak form-factors for heavy meson decays: An update, Phys. Rev. D **62**, 014006 (2000).
[53] C. Q. Geng, C.-W. Hwang, C. C. Lih, and W. M. Zhang, Mesonic tensor form-factors with light front quark model, Phys. Rev. D **64**, 114024 (2001).
[54] C.-D. Lu, W. Wang, and Z.-T. Wei, Heavy-to-light form factors on the light cone, Phys. Rev. D **76**, 014013 (2007).
[55] C. Albertus, Weak decays of $\bar{B}_s$ mesons, Phys. Rev. D **89**, 065042 (2014).
[56] H.-Y. Cheng, C.-K. Chua, and C.-W. Hwang, Covariant light front approach for s wave and p wave mesons: Its application to decay constants and form-factors, Phys. Rev. D **69**, 074025 (2004).
[57] H.-Y. Cheng and C.-K. Chua, B to V, A, T tensor form factors in the covariant light-front approach: Implications on radiative B decays, Phys. Rev. D **81**, 114006 (2010); **82**, 059904(E) (2010).
[58] C.-H. Chen, Y.-L. Shen, and W. Wang, $|V_{ub}|$ and $B \to \eta^{(\prime)}$ form factors in covariant light front approach, Phys. Lett. B **686**, 118 (2010).
[59] A. Bharucha, D. M. Straub, and R. Zwicky, $B \to V\ell^+\ell^-$ in the standard model from light-cone sum rules, J. High Energy Phys. 08 (2016) 098.
[60] P. Ball and V. M. Braun, Exclusive semileptonic and rare B meson decays in QCD, Phys. Rev. D **58**, 094016 (1998).
[61] P. Ball, $B \to \pi$ and $B \to K$ transitions from QCD sum rules on the light cone, J. High Energy Phys. 09 (1998) 005.
[62] P. Ball and R. Zwicky, Improved analysis of $B \to \pi e\nu$ from QCD sum rules on the light cone, J. High Energy Phys. 10 (2001) 019.
[63] P. Ball and R. Zwicky, New results on $B \to \pi, K, \eta$ decay formfactors from light-cone sum rules, Phys. Rev. D **71**, 014015 (2005).
[64] P. Ball and R. Zwicky, $B_{d,s} \to \rho, \omega, K^*, \phi$ decay form-factors from light-cone sum rules revisited, Phys. Rev. D **71**, 014029 (2005).
[65] P. Ball and G. W. Jones, $B \to \eta^{(\prime)}$ form factors in QCD, J. High Energy Phys. 08 (2007) 025.
[66] J. Charles, A. Le Yaouanc, L. Oliver, O. Pene, and J. C. Raynal, Heavy to light form-factors in the heavy mass to large energy limit of QCD, Phys. Rev. D **60**, 014001 (1999).
[67] A. Bharucha, T. Feldmann, and M. Wick, Theoretical and phenomenological constraints on form factors for radiative and semi-leptonic B-meson decays, J. High Energy Phys. 09 (2010) 090.
[68] A. Bharucha, $B \to \pi$ form factor from QCD sum rules on the light-cone and $|V_{ub}|$, J. High Energy Phys. 05 (2012) 092.
[69] A. Khodjamirian, T. Mannel, and N. Offen, Form-factors from light-cone sum rules with B-meson distribution amplitudes, Phys. Rev. D **75**, 054013 (2007).
[70] A. Khodjamirian, T. Mannel, N. Offen, and Y. M. Wang, $B \to \pi\ell\nu_l$ width and $|V_{ub}|$ from QCD light-cone sum rules, Phys. Rev. D **83**, 094031 (2011).
[71] Y.-M. Wang and Y.-L. Shen, QCD corrections to $B \to \pi$ form factors from light-cone sum rules, Nucl. Phys. **B898**, 563 (2015).
[72] U.-G. Meißner and W. Wang, Generalized heavy-to-light form factors in light-cone sum rules, Phys. Lett. B **730**, 336 (2014).
[73] Y.-L. Wu, M. Zhong, and Y.-B. Zuo, $B_{(s)}$, $D_{(s)} \to \pi, K, \eta, \rho, K^*, \omega, \phi$ transition form factors and decay rates with extraction of the CKM parameters $|V_{ub}|$, $|V_{cs}|$, $|V_{cd}|$, Int. J. Mod. Phys. A **21**, 6125 (2006).
[74] X.-G. Wu and T. Huang, Radiative corrections on the $B \to P$ form factors with chiral current in the light-cone sum rules, Phys. Rev. D **79**, 034013 (2009).
[75] M. A. Ivanov, J. G. Korner, S. G. Kovalenko, P. Santorelli, and G. G. Saidullaeva, Form factors for semileptonic, nonleptonic and rare $B(B_s)$ meson decays, Phys. Rev. D **85**, 034004 (2012).
[76] M. Ahmady, R. Campbell, S. Lord, and R. Sandapen, Predicting the $B \to K^*$ form factors in light-cone QCD, Phys. Rev. D **89**, 074021 (2014).

[77] H.-B. Fu, X.-G. Wu, and Y. Ma, $B \to K^*$ transition form factors and the semi-leptonic decay $B \to K^*\mu^+\mu^-$, J. Phys. G **43**, 015002 (2016).

[78] J. Gao, C.-D. Lü, Y.-L. Shen, Y.-M. Wang, and Y.-B. Wei, Precision calculations of $B \to V$ form factors from soft-collinear effective theory sum rules on the light-cone, Phys. Rev. D **101**, 074035 (2020).

[79] B.-Y. Cui, Y.-K. Huang, Y.-L. Shen, C. Wang, and Y.-M. Wang, Precision calculations of $B_{d,s} \to \pi, K$ decay form factors in soft-collinear effective theory, J. High Energy Phys. 03 (2023) 140.

[80] H.-n. Li, Y.-L. Shen, and Y.-M. Wang, Next-to-leading-order corrections to $B \to \pi$ form factors in k_T factorization, Phys. Rev. D **85**, 074004 (2012).

[81] W.-F. Wang and Z.-J. Xiao, The semileptonic decays $B/B_s \to (\pi, K)(\ell^+\ell^-, \ell\nu, \nu\bar{\nu})$ in the perturbative QCD approach beyond the leading-order, Phys. Rev. D **86**, 114025 (2012).

[82] W.-F. Wang, Y.-Y. Fan, M. Liu, and Z.-J. Xiao, Semileptonic decays $B/B_s \to (\eta, \eta', G)(l^+l^-, l\bar{\nu}, \nu\bar{\nu})$ in the perturbative QCD approach beyond the leading order, Phys. Rev. D **87**, 097501 (2013).

[83] Y.-Y. Fan, W.-F. Wang, S. Cheng, and Z.-J. Xiao, Semileptonic decays $B \to D^{(*)}l\nu$ in the perturbative QCD factorization approach, Chin. Sci. Bull. **59**, 125 (2014).

[84] Y.-Y. Fan, W.-F. Wang, and Z.-J. Xiao, Study of $\bar{B}_s^0 \to (D_s^+, D_s^{*+})l^-\bar{\nu}_l$ decays in the pQCD factorization approach, Phys. Rev. D **89**, 014030 (2014).

[85] T. Kurimoto, H.-n. Li, and A. I. Sanda, Leading power contributions to $B \to \pi, \rho$ transition form-factors, Phys. Rev. D **65**, 014007 (2002).

[86] C.-D. Lu and M.-Z. Yang, B to light meson transition form-factors calculated in perturbative QCD approach, Eur. Phys. J. C **28**, 515 (2003).

[87] Z.-T. Wei and M.-Z. Yang, The systematic study of $B \to \pi$ form-factors in pQCD approach and its reliability, Nucl. Phys. **B642**, 263 (2002).

[88] T. Huang and X.-G. Wu, Consistent calculation of the B to π transition form-factor in the whole physical region, Phys. Rev. D **71**, 034018 (2005).

[89] R. R. Horgan, Z. Liu, S. Meinel, and M. Wingate, Lattice QCD calculation of form factors describing the rare decays $B \to K^*\ell^+\ell^-$ and $B_s \to \phi\ell^+\ell^-$, Phys. Rev. D **89**, 094501 (2014).

[90] E. Dalgic, A. Gray, M. Wingate, C. T. H. Davies, G. P. Lepage, and J. Shigemitsu, B meson semileptonic form-factors from unquenched lattice QCD, Phys. Rev. D **73**, 074502 (2006); **75**, 119906(E) (2007).

[91] S. Aoki *et al.*, Review of lattice results concerning low-energy particle physics, Eur. Phys. J. C **74**, 2890 (2014).

[92] H.-n. Li, S. Mishima, and A. I. Sanda, Resolution to the $B \to \pi K$ puzzle, Phys. Rev. D **72**, 114005 (2005).

[93] H.-Y. Cheng and C.-K. Chua, Charmless three-body decays of B_s mesons, Phys. Rev. D **89**, 074025 (2014).

[94] B. Aubert *et al.* (*BABAR* Collaboration), Evidence for direct CP violation from Dalitz-plot analysis of $B^\pm \to K^\pm\pi^\mp\pi^\pm$, Phys. Rev. D **78**, 012004 (2008).

[95] J. P. Lees *et al.* (*BABAR* Collaboration), Observation of the rare decay $B^+ \to K^+\pi^0\pi^0$ and measurement of the quasi-two body contributions $B^+ \to K^*(892)^+\pi^0$, $B^+ \to f_0(980)K^+$ and $B^+ \to \chi_{c0}K^+$, Phys. Rev. D **84**, 092007 (2011).

[96] B. Aubert *et al.* (*BABAR* Collaboration), Time-dependent amplitude analysis of $B^0 \to K_S^0\pi^+\pi^-$, Phys. Rev. D **80**, 112001 (2009).

[97] A. Garmash *et al.* (Belle Collaboration), Evidence for Large Direct CP Violation in $B \pm \rho(770)^0K^\pm$ from Analysis of the Three-Body Charmless $B^\pm \to K^\pm\pi^\pm\pi^\mp$ Decay, Phys. Rev. Lett. **96**, 251803 (2006).

[98] P. Chang *et al.* (Belle Collaboration), Observation of the decays $B^0 \to K^+\pi^-\pi^0$ and $B^0 \to \rho^-K^+$, Phys. Lett. B **599**, 148 (2004).

[99] J. P. Lees *et al.* (*BABAR* Collaboration), Study of CP violation in Dalitz-plot analyses of $B^0 \to K^+K^-K_S^0$, $B^+ \to K^+K^-K^+$, and $B^+ \to K_S^0K_S^0K^+$, Phys. Rev. D **85**, 112010 (2012).

[100] A. Garmash *et al.* (Belle Collaboration), Dalitz analysis of the three-body charmless decays $B^+ \to K^+\pi^+\pi^-$ and $B^+ \to K^+K^+K^-$, Phys. Rev. D **71**, 092003 (2005).

[101] R. Aaij *et al.* (LHCb Collaboration), Amplitude Analysis of $B^\pm \to \pi^\pm K^+K^-$ Decays, Phys. Rev. Lett. **123**, 231802 (2019).

[102] C. L. Hsu *et al.* (Belle Collaboration), Measurement of branching fraction and direct CP asymmetry in charmless $B^+ \to K^+K^-\pi^+$ decays at Belle, Phys. Rev. D **96**, 031101 (2017).

[103] B. Aubert *et al.* (*BABAR* Collaboration), Observation of the Decay $B^+ \to K^+K^-\pi^+$, Phys. Rev. Lett. **99**, 221801 (2007).